

# ENERGY LEVELS, LIFETIMES AND TRANSITION RATES FOR P-LIKE IONS FROM Cr X TO Zn XVI FROM LARGE-SCALE RELATIVISTIC MULTICONFIGURATION CALCULATIONS

K. WANG<sup>1,2,3</sup>, P. JÖNSSON<sup>1</sup>, G. GAIGALAS<sup>4</sup>, L. RADŽIŪTĖ<sup>4</sup>, P. RYNKUN<sup>4</sup>, G. DEL ZANNA<sup>5</sup>, C. Y. CHEN<sup>3</sup>

<sup>1</sup>Group for Materials Science and Applied Mathematics, Malmö University, SE-20506, Malmö, Sweden; [per.jonsson@mah.se](mailto:per.jonsson@mah.se)

<sup>2</sup>Hebei Key Lab of Optic-electronic Information and Materials, The College of Physics Science and Technology, Hebei University, Baoding 071002, China

<sup>3</sup>Shanghai EBIT Lab, Institute of Modern Physics, Department of Nuclear Science and Technology, Fudan University, Shanghai 200433, China; [chychen@fudan.edu.cn](mailto:chychen@fudan.edu.cn)

<sup>4</sup>Institute of Theoretical Physics and Astronomy, Vilnius University, Saulėtekio av. 3, LT-10222, Vilnius, Lithuania

<sup>5</sup>DAMTP, Centre for Mathematical Sciences, University of Cambridge, Wilberforce Road, Cambridge CB3 0WA, UK

## ABSTRACT

The fully relativistic multiconfiguration Dirac–Hartree–Fock method is used to compute excitation energies and lifetimes for the 143 lowest states of the  $3s^23p^3$ ,  $3s3p^4$ ,  $3s^23p^23d$ ,  $3s3p^33d$ ,  $3p^5$ ,  $3s^23p3d^2$  configurations in P-like ions from Cr X to Zn XVI. Multipole (E1, M1, E2, M2) transition rates, line strengths, oscillator strengths, and branching fractions among these states are also given. Valence-valence and core-valence electron correlation effects are systematically accounted for using large basis function expansions. Computed excitation energies are compared with the NIST ASD and CHIANTI compiled values and previous calculations. The mean average absolute difference, removing obvious outliers, between computed and observed energies for the 41 lowest identified levels in Fe XII is only 0.057 %, implying that the computed energies are accurate enough to aid identification of new emission lines from the sun and other astrophysical sources. The amount of energy and transition data of high accuracy is significantly increased for several P-like ions of astrophysics interest, where experimental data are still very scarce.

*Keywords:* atomic data - atomic processes

## 1. INTRODUCTION

P-like ions of the iron group elements have prominent lines in the ultraviolet (UV) and extreme ultraviolet (EUV) spectral regions that are used for plasma diagnostics, especially to measure electron densities. Fe XII is especially important for the solar corona, as it produces the most prominent lines in the EUV, as observed by e.g. Skylab, SOHO, and more recently with the EUV Imaging Spectrometer (EIS) instrument on board the Hinode satellite (see, e.g. [Young et al. 2009](#); [Del Zanna 2012](#)). Fe XII lines have also been observed by Chandra and XMM-Newton ([Raassen et al. 2002](#)).

Because of their complex atomic structure, the radiative and scattering (by electron impact) calculations of P-like ions are notoriously difficult. Because of its importance, much effort has been produced to provide accurate scattering data for Fe XII, see for example [Storey et al. \(2005\)](#); [Del Zanna et al. \(2012\)](#). It is only with the most recent calculations that large discrepancies between predicted and observed line emission has largely been resolved. Only about half of the  $3s^23p^23d$  levels in Fe XII were identified, mostly by

B.C.Fawcett and collaborators (cf. [Bromage et al. 1978](#)) in the 1970’s, from the strongest decays in the EUV observed in theta-pinch spectra. [Del Zanna & Mason \(2005\)](#) reviewed the identifications and suggested several new ones, using the [Storey et al. \(2005\)](#) atomic data.

Important information for some of the states of the  $3s^23p^23d$  configuration has been obtained from fast-beam spectroscopy. For example, radiative lifetimes in Fe XII, Co XIII and Cu XV were measured by [Träbert \(1998\)](#). For a recent review on Fe XII see [Träbert et al. \(2008\)](#). As noted by [Vilkas & Ishikawa \(2004\)](#), there are however some differences between calculated and measured lifetimes, calling for a reexamination of the latter.

Much effort has also been devoted to the calculation of radiative data for Fe XII, also to aid the identifications (see, e.g. [Froese Fischer et al. 2006](#); [Vilkas & Ishikawa 2004](#); [Tayal 2011](#)). The identifications and atomic data for the Fe XII lines have recently been reviewed by [Beiersdorfer et al. \(2014a\)](#) using EBIT spectroscopic measurements, noting one significant discrepancy with the identifications proposed by [Del Zanna & Mason \(2005\)](#).

For the other P-like ions, very few atomic data are available, with the exception of a few low charge states and Ni XIV. Although less studied, also Ni XIV has diagnostic value and atomic data - electron impact collision strengths, energy levels, oscillator strengths, and spontaneous radiative decay rates - have been calculated by [Landi & Bhatia \(2010\)](#).

The purpose of the present work is to provide transition energies for the lowest 143 states in P-like ions with spectroscopic accuracy, i.e. the accuracy is high enough so that the energies can be directly used to identify lines from laboratory or space observations. Further, the present work aims at providing a consistent and accurate set of transition rates for all the ions, for modeling purposes. This work is an extension of our previous efforts ([Chen et al. 2018, 2017](#); [Guo et al. 2016](#); [Guo et al. 2015](#); [Jönsson et al. 2014, 2013](#); [Jönsson et al. 2011](#); [Wang et al. 2018a,b, 2017a,b,c,d, 2016a,b, 2015, 2014](#); [Si et al. 2017, 2016](#); [Zhao et al. 2017](#)) to supply highly accurate atomic data for L- and M-shell systems, see [Jönsson et al. \(2017\)](#) for a review.

## 2. THEORY AND CALCULATIONS

### 2.1. MCDHF

In the multiconfiguration Dirac-Hartree-Fock (MCDHF) method the wave function  $\Psi(\gamma PJM)$  for a state labeled  $\gamma PJM$ , where  $\gamma$  is the orbital occupancy and angular coupling tree quantum numbers,  $P$  the parity,  $J$  the total angular momentum quantum number, and  $M$  the total magnetic quantum number, is written as a linear combination of  $N$  configuration state functions  $\Phi(\gamma_r PJM)$  (CSFs)

$$\Psi(\gamma PJM) = \sum_{r=1}^N c_r \Phi(\gamma_r PJM). \quad (1)$$

The CSFs are antisymmetrized and  $jj$ -coupled many electron functions built from products of one-electron Dirac orbitals ([Grant 2007](#); [Froese Fischer et al. 2016](#)). The radial parts of the Dirac orbitals and the expansion coefficients for the targeted states are obtained by solving the MCDHF equations, which result from applying the stationary condition on the state averaged Dirac-Coulomb energy functional with added terms to enforce orthonormality of the radial orbitals. The Breit interaction and leading QED effects (vacuum polarization and self-energy) are included in subsequent configuration interaction (CI) calculations.

### 2.2. Transition parameters

Transition parameters such as transition rates  $A$ , line strengths  $S$ , and weighted oscillator strengths  $gf$  between an initial  $\gamma PJM$  and a final  $\gamma' P' J' M'$  state are

expressed in terms of reduced matrix elements

$$\langle \Psi(\gamma PJ) \| \mathbf{T} \| \Psi(\gamma' P' J') \rangle = \sum_{r,s} c_r c'_s \langle \Phi(\gamma_r PJ) \| \mathbf{T} \| \Phi(\gamma'_s P' J') \rangle, \quad (2)$$

where  $\mathbf{T}$  is the transition operator. The evaluation of the matrix elements between separately optimized initial and final states, i.e. states that are built from different and mutually non-orthonormal orbital sets, follows the prescription given in [Olsen et al. \(1995\)](#).

For electric multipole transitions E1, E2 etc. there are two forms of the transition operator; the length (Babushkin) form and the velocity (Coulomb) form ([Grant 1974](#)). The length form is usually preferred. Following [Froese Fischer \(2009\)](#) and [Ekman et al. \(2014\)](#) we use the relative difference

$$dT = \frac{|A_l - A_v|}{\max(A_l, A_v)} \quad (3)$$

of the transition rates  $A_l$  and  $A_v$  computed in length and velocity form as an indicator of accuracy of the rate. It should be emphasized that the values of  $dT$  do not represent an uncertainty estimate of the rate for each individual transition. Instead, they should be considered statistical indicators of uncertainties within given sets of transitions.

### 2.3. Calculations

Calculations were performed for the 143 lowest states belonging to the  $3s^2 3p^3$ ,  $3p^5$ ,  $3s 3p^3 3d$  odd and  $3s 3p^4$ ,  $3s^2 3p^2 3d$ ,  $3s 3p^2 3d^2$  even configurations. The odd and even states were determined in separate calculations. As a starting point, two MCDHF calculations were performed for, respectively, the statistically weighted average of the odd and even parity states. To include electron correlation, and improve on the computed energies and wave functions, the initial calculations were followed by separate MCDHF calculations for the odd and even parity states, with CSF expansions obtained by allowing single and double (SD) substitutions from the reference configurations to active orbital sets with principal quantum numbers up to  $n = 6$  and with orbital angular momenta up to  $l = 5$  ( $h$ -orbitals). Only CSFs that have non-zero matrix elements with the CSFs belonging to the reference configurations were retained. No substitutions were allowed from the  $1s$  shell, which defines an inactive closed core. Furthermore, the substitutions were restricted in such a way that only one substitution was allowed from the  $2s$  and  $2p$  subshells of the configurations in the MR, and thus the generated expansions account for valence and core-valence electron correlation ([Sturesson et al. 2007](#); [Froese Fischer et al. 2016](#)). The wave functions were further improved by augmenting the above expansions with CSFs obtained by SD substitutions from the valence subshells of the

reference configurations to active orbital sets with principal quantum numbers extended to  $n = 8$  and with orbital angular momenta up to  $l = 6$ . The neglected core-core correlation is comparatively unimportant for both the energy separations and the transition probabilities (Gustafsson et al. 2017).

The MCDHF calculations were followed by CI calculations including the Breit-interaction and leading QED effects. The number of CSFs in the final odd and even state expansions were approximately 3 250 000 and 4 600 000, respectively, distributed over the different  $J$  symmetries. All calculations were performed with the GRASP2K code (Jönsson et al. 2007; Jönsson et al. 2013). To provide the  $LSJ$  labeling system used in databases such as the NIST ASD (Kramida et al. 2018) and CHIANTI (Del Zanna et al. 2015; Dere et al. 1997), the wave functions are transformed from a  $jj$ -coupled CSF basis into a  $LSJ$ -coupled CSF basis using the methods developed by Gaigalas (Gaigalas et al. 2004; Gaigalas et al. 2017).

### 3. EVALUATION OF DATA

#### 3.1. Energy Levels and Lifetimes

The excitation energies and lifetimes for the 143 lowest states of Fe XII from the largest CI calculation with orbital sets with principal quantum numbers up to  $n = 8$  and with orbital angular momenta up to  $l = 6$  are displayed in Table 1. For comparison, compiled excitation energies from NIST ASD (Kramida et al. 2018) and compiled and calculated energies from CHIANTI version 8 (Del Zanna et al. 2015; Dere et al. 1997) are also given along with excitation energies from the MR-MP calculations by Vilkas & Ishikawa (2004), MCHF-BP with non-orthogonal orbitals by Tayal (2011) and superstructure (SS) calculations by Storey et al. (2005). Lifetimes from CHIANTI as well as from the three latter calculations are also given. We note that the CHIANTI v.8 data were obtained by Del Zanna et al. (2012) with semi-empirical corrections. The agreement between the present MCDHF/CI calculations and observations is, although not as excellent as for the MR-MP calculation by Vilkas, very good. Also the calculations by Tayal reproduce the excitation energies to a high degree. The SS calculations, which mainly aim at providing target states for scattering calculations, are semi-empirically scaled. For the states where there are no experimental data, the SS calculations differ strongly from the more accurate MCDHF/CI and MR-MP calculations.

For P-like ions the ground state is a quartet state, and it is known that high spin states converge more rapidly with respect to the increasing orbital space than the other states (Gálvez et al. 2005; Jönsson et al. 2017). As a consequence there is a energy shift in the

MCDHF/CI calculations so that the excited states are somewhat too high relative to the ground state. To quantify the shift we computed the mean level deviation,  $MLD$ , according to

$$MLD = \frac{1}{N} \sum_{i=1}^N |E_{obs}(i) - E_{cal}(i) + ES|, \quad (4)$$

where  $N$  is the number of states. The energy shift,  $ES$ , is chosen as to minimize the sum. For MCDHF/CI we have a shift  $ES = 367 \text{ cm}^{-1}$  and  $MLD = 213 \text{ cm}^{-1}$ . The corresponding values for MR-MP and the MCHF-BP calculations are  $ES = 233 \text{ cm}^{-1}$  and  $MLD = 271 \text{ cm}^{-1}$  and  $ES = 500 \text{ cm}^{-1}$  and  $MLD = 3993 \text{ cm}^{-1}$ , respectively. Thus the spread for the MCDHF/CI calculation is small. By subtracting  $ES$  from the energies of the excited states we greatly improve the predictive power of the calculated values, facilitating the use of the transition energies for identifying lines in observed spectra. The mean level deviation  $ES$  analysis is summarized in Table 2.

Turning to the lifetimes we compare our lifetimes with theoretical lifetimes in the CHIANTI database (Del Zanna et al. 2015; Dere et al. 1997) and lifetimes from the calculations by Tayal (2011) and Vilkas & Ishikawa (2004). The latter two calculations only include the E1 transitions, and thus there are no lifetimes for the states of the ground term, nor from states 18 and 25. The MCDHF/CI lifetimes are computed in both the length form and velocity form. Excluding the states of the ground term configuration and 18 and 25, which are governed by higher multipoles, the lifetimes in the two forms agrees to within 0.3 % in mean. This agreement is highly satisfactory and indicate accurate values (Ekman et al. 2014). The consistency of the calculated lifetimes from the different methods is fair, but with clear anomalies for some states; for state 23 the lifetimes varies between  $1.0 \times 10^{-4} \text{ s}$  and  $5.4 \times 10^{-6} \text{ s}$ . Comparing with the experimental lifetimes of Träbert (1998) we see that the calculated lifetimes for state 19 all gather around  $3.0 \times 10^{-8} \text{ s}$ , which is about a factor of four longer than the experimental value  $7.3 \pm 1 \times 10^{-9} \text{ s}$ . Large differences between calculated and experimental lifetimes are also found for states in Co XIII and Cu XV. New experiments are needed to clarify these differences.

In Table 3 (the full table is available on-line) we give calculated excitations energies as well as energies shifted according to the  $ES$  values from a mean level deviation analysis that is summarized in Table 2. For comparison, excitation energies from Sugar & Corliss (1985); Cr X, Mn XI, Fe XII, Co XIII, Ni XIV, Sugar & Musgrove (1990); Cu XV, Sugar & Musgrove (1995); Zn XVI, compiled and reported in NIST ASD, are also given

as well as excitation energies from the MR-MP calculations by [Vilkas & Ishikawa \(2004\)](#). We can see excellent agreement in all the cases where an experimental energy is available (except for Fe XII, see below). The excitation energies from the shifted energies are estimated to be accurate to within 0.05 % and are therefore helpful in identifying transitions in spectra from laboratory and astrophysical spectra. Finally, the table gives the calculated lifetimes in the length and velocity gauges, where the former values are generally believed to be more accurate.

### 3.2. Fe XII line identifications

Table 4 lists our shifted energies for the 41 lowest Fe XII levels ( $3s^23p^3$ ,  $3s3p^4$ ,  $3s^23p^23d$ ), compared with three sets of experimental data: those in the NIST database, those suggested by [Del Zanna & Mason \(2005\)](#) and those available in the CHIANTI database version 8 ([Del Zanna et al. 2015](#)). The NIST energies are mainly originating from laboratory measurements of B.C. Fawcett and collaborators in the 1970s (see, e.g. [Bromage et al. 1978](#)). [Del Zanna & Mason \(2005\)](#) used available astrophysical spectra, in addition to Fawcett’s laboratory plates and semi-empirically adjusted theoretical energies, to suggest new identifications of almost all the previously-unknown  $3s^23p^23d$  levels. Aside from two exceptions, we can see from Table 4 an excellent agreement between the present energies and those listed by [Del Zanna & Mason \(2005\)](#), in terms of both the suggested experimental energies and the predicted ones, for the  $3s^23p^23d$  levels.

Later, [Del Zanna \(2012\)](#) presented a table of wavelengths and calibrated radiances of coronal lines observed off the solar limb with Hinode EIS. On the basis of these observations, two new Fe XII identifications were suggested, and later introduced in CHIANTI version 8. The first one is the main decay from the  $3s^23p^23d\ ^4D_{3/2}$  (level 21). It was tentatively assigned to a self-blend at 249.38 Å, changing the predicted energy from 448071  $\text{cm}^{-1}$  (which is very close to our predicted one) to 447076  $\text{cm}^{-1}$ . Our energy predicts that the line should be at 248.56 Å. There is indeed a weak line in the coronal EIS spectrum observed at 248.50 Å. The observed intensity, relative to the other Fe XII known lines, is in broad agreement with the theoretical ratio, according to CHIANTI version 8. This weak line would normally be blended with an O V transition in on-disk observations. However, the observations of [Del Zanna \(2012\)](#) were off-limb where no emission in low-temperature lines such O V was present. Therefore, it is likely that this is the correct assignment.

The second tentative identification from [Del Zanna \(2012\)](#) regards the main decay from the  $3s^23p^23d\ ^4D_{5/2}$  (level 22), with a weak coronal line observed at 245.89 Å.

In this case the experimental energy is almost the same (452775  $\text{cm}^{-1}$ ) as our predicted one (452671  $\text{cm}^{-1}$ ), so it appears that this tentative identification is correct.

Finally, the main discrepancy with the [Del Zanna & Mason \(2005\)](#) identifications regards the  $3s^23p^23d\ ^2S_{1/2}$  (level 38), which has a large difference (3674  $\text{cm}^{-1}$ ) with our predicted value. Its main decay, to the  $3s^23p^3\ ^2P_{3/2}$  level, is a transition which becomes strong at high densities. On the basis of their estimated energy for this level, [Del Zanna & Mason \(2005\)](#) assigned this decay to a previously unidentified line present in the laboratory plates at 201.76 Å. On the other hand, the original NIST energy was 579630  $\text{cm}^{-1}$ , i.e. very close to our predicted energy (579827  $\text{cm}^{-1}$ ) and to the value (579853  $\text{cm}^{-1}$ ) from the MR-MP calculations by [Vilkas & Ishikawa \(2004\)](#). The NIST energy originated from the identification, on the same laboratory plates, with the 200.356 Å line by [Bromage et al. \(1978\)](#).

It is clear that the original identification by Bromage et al. was correct. Indeed, this issue was pointed out by [Beiersdorfer et al. \(2014b\)](#). Excellent agreement was found between the EBIT spectrum and the CHIANTI atomic data, which included the [Del Zanna & Mason \(2005\)](#) identifications for P-like Fe and similar ones obtained by Del Zanna on a number of other coronal iron ions. Only one main exception stood out, the line at 200.356 Å, which is strong in the EBIT spectra.

Regarding the  $3s3p^33d$  levels, we note that none of them were previously identified with certainty. Lines within the  $3s3p^4$ - $3s3p^33d$  transition array are in fact much weaker compared to the decays from the  $3s^23p^23d$  levels. The strongest decay, the dipole-allowed  $^4P_{5/2}$ - $^4D_{7/2}$  line (transition 6–84) was tentatively identified by [Del Zanna & Mason \(2005\)](#) with the 191.045 Å line, although later estimates of the energies by [Del Zanna et al. \(2012\)](#) put this identification in doubt. The present *ab initio* energy for the upper level is 810021  $\text{cm}^{-1}$ . Applying the same ES shift of Table 2 (367  $\text{cm}^{-1}$ ), we predict the decay to be at 186.8 Å. Considering the intensity of this decay and the Hinode EIS observations ([Del Zanna 2012](#)), there are only two possibilities close in wavelength: the first is the 186.88 Å line, which is already a known blend of three transitions (two already from Fe XII); the second is the 187.00 Å line. It is very much likely that the second possibility is the correct identification, given that the 187.00 Å line is currently unidentified and has an observed intensity close to the predicted one (according to CHIANTI version 8), relative to the intensities of the known Fe XII lines. The energy of the upper level would then be only 522  $\text{cm}^{-1}$  lower than our prediction. Moreover, the second strongest transition from these levels is the decay from the close  $3s3p^33d\ ^4D_{5/2}$  (level 87) to the  $3s3p^4\ ^4P_{3/2}$



(level 7). Applying the same shift of  $522 \text{ cm}^{-1}$  to this  $^4D_{5/2}$  upper level, we find a wavelength of  $189.08 \text{ \AA}$ , very close to an observed coronal line at  $189.12 \text{ \AA}$ , identified by [Del Zanna \(2012\)](#) as an Fe XI transition which was significantly (50 %) blended. The predicted intensity of the Fe XII transition would explain the blend. If we assumed that the 6–84 transition would blend the  $186.88 \text{ \AA}$  line, we would expect the 7–87 transition to fall at  $189.0 \text{ \AA}$ , where there is a coronal line, but its intensity is entirely due to Fe XI, as shown in [Del Zanna \(2012\)](#). Finally, a weaker decay of level 87 to level 6 ( $3s3p^4 \ ^4P_{5/2}$ ) should also be observable by Hinode EIS at  $185.70 \text{ \AA}$ , assuming the second option (with a shift of  $522 \text{ cm}^{-1}$ ). Indeed there is a weak coronal unidentified line at  $185.68 \text{ \AA}$ .

Another  $3s3p^33d$  level which should produce a weak but observable line is the lower  $^4D_{7/2}$  (level 50), with a decay to the  $3s^23p^23d \ ^4P_{5/2}$  (level 27). Its predicted intensity, using the [Del Zanna et al. \(2012\)](#) atomic data, is about 1/10 the intensity of the decay of the  $3s^23p^23d \ ^4F_{9/2}$  (the 6–18 transition), identified by [Del Zanna & Mason \(2005\)](#) with the  $592.6 \text{ \AA}$  line. Our predicted energy, with the  $367 \text{ cm}^{-1}$  adjustment, predicts this decay to be at  $592.7 \text{ \AA}$ . Given that there are no other obvious coronal lines nearby, and the fact that the intensity of the 6–18 transition was only able to explain about 70 % of the observed intensity ([Del Zanna & Mason 2005](#)), plus the fact that this line is broader than the other nearby coronal lines, we conclude that it is very likely that the 27–50 transition is blending the  $592.6 \text{ \AA}$  line.

### 3.3. Transition rates

In [Table 5](#) (the full table is available on-line), wavelengths, transition rates  $A_{ji}$ , weighted oscillator strengths  $gf_{ji}$  and line strength  $S_{ji}$ , the latter in the length form, are given along with branching fractions ( $BF_{ji} = \frac{A_{ji}}{\sum_{k=1}^{j-1} A_{jk}}$ ) and the uncertainty indicator  $dT$ . For most of the stronger E1 transitions  $dT$  is well below 5 %. For the weaker transitions, as displayed in the scatterplot of  $dT$  versus the line strength  $S$  for transitions in Fe XII with branching fractions  $BF > 1 \%$ , the uncertainty  $dT$  is somewhat larger, from 5 % percent up to 30 % ([Figure 1](#)). The weaker E1 transitions are often intercombination transitions, where the smallness of the rates comes from cancellations in the contributions to the transition matrix elements, compare [Ynnerman & Fischer \(1995\)](#), or two-electron-one-photon transitions, which have zero rate in the lowest approximation and where the transition is opened as corrective basis functions are included in the wave function expansions ([Li et al. 2010](#)). These two types of transitions are still challenging to theory, requiring very large

CSF expansions.

In [Table 6](#), our calculate transition rates and wavelengths for the brightest coronal lines in Fe XII are compared with the values given by [Del Zanna & Mason \(2005\)](#) and NIST. There is a good agreement between the current transition rates and the rates given by [Del Zanna & Mason \(2005\)](#). There are however a few noticeable differences: for line 3 - 23 the rate from the current calculation is almost three times larger than the one from [Del Zanna & Mason \(2005\)](#), for 2 - 30 the value from the current calculations agrees reasonably well with the value from [Del Zanna & Mason \(2005\)](#), both being more than two times larger than the value given by NIST. Looking at the wavelengths we see that the current calculation provide excellent predictions. For the last transition (6 - 84) there is a noticeable difference with the wavelength by [Del Zanna & Mason \(2005\)](#), as we have previously discussed.

## 4. SUMMARY AND CONCLUSIONS

We have performed MCDHF and subsequent CI calculations including Breit and QED effects for states of the  $3s^23p^3$ ,  $3s3p^4$ ,  $3s^23p^23d$ ,  $3s3p^33d$ ,  $3p^5$ ,  $3s^23p3d^2$  configurations in P-like ions from Cr X to Zn XVI. Valence-valence and core-valence electron correlation effects are included in large basis expansions. Excitation energies, lifetimes, and transition rates are given. Energies from the CI calculations are in overall excellent agreement with the few observations available for the  $3s^23p^3$ ,  $3s3p^4$ ,  $3s^23p^23d$  levels. It is clear that the computed wavelengths are accurate enough to directly aid line identification in the spectra. In particular, we have reassessed the previous identifications of the important Fe XII  $3s^23p^23d$  levels, confirming most of the previous suggestions. We have also suggested new identifications of a few  $3s3p^33d$  levels, on the basis of our calculated energies, Hinode EIS spectra and the [Del Zanna et al. \(2012\)](#) atomic data. Further work on the other ions in the sequence is in progress, to see if more spectral lines can be identified.

Uncertainties of the transition rates are estimated by the relative difference  $dT$  between the values in length and velocity form. For most of the stronger transitions  $dT$  is well below 5 %. For the weaker transitions the uncertainty  $dT$  is somewhat larger, from 5 % up to 30 %. We are therefore confident that the transition rates are highly accurate. Data from the present study will serve as a benchmark for further calculations.

We acknowledge the support from the National Key Research and Development Program of China under Grant No. 2017YFA0402300, the National Natural Science Foundation of China (Grant Grant No. 11703004 and No. 11674066) and the Nature Science Foundation

of Hebei Province, China (A2017201165). This work is also supported by the Swedish research council under contract 2015-04842. K.W. expresses his gratitude for the support from the visiting researcher program at the Fudan University. G. D. Z. acknowledges the support from STFC (UK) through the consolidated grant RG 84192.

*Software:* GRASP2K ([Jönsson et al. 2007](#); [Jönsson et al. 2013](#)) is used in the present work.

## REFERENCES

- Beiersdorfer, P., Lepson, J. K., Desai, P., Díaz, F., & Ishikawa, Y. 2014a, *ApJS*, 210, 16
- Beiersdorfer, P., Träbert, E., Lepson, J. K., Brickhouse, N. S., & Golub, L. 2014b, *Astrophys. J.*, 788, 25
- Bromage, G. E., Fawcett, B. C., & Cowan, R. D. 1978, *MNRAS*, 183, 19
- Chen, Z. B., Guo, X. L., & Wang, K. 2018, *JQSRT*, 206, 213
- Chen, Z. B., Ma, K., Wang, H. J., et al. 2017, *ADNDT*, 113, 258
- Del Zanna, G. 2012, *A&A*, 537, A38
- Del Zanna, G., Dere, K. P., Young, P. R., Landi, E., & Mason, H. E. 2015, *A&A*, 582, A56
- Del Zanna, G., & Mason, H. E. 2005, *A&A*, 433, 731
- Del Zanna, G., Storey, P. J., Badnell, N. R., & Mason, H. E. 2012, *A&A*, 543, A139
- Dere, K. P., Landi, E., Mason, H. E., Monsignori Fossi, B. C., & Young, P. R. 1997, *A&AS*, 125, 149
- Ekman, J., Godefroid, M. R., & Hartman, H. 2014, *Atoms*, 2, 215
- Froese Fischer, C. 2009, *PhyS*, T134, 014019
- Froese Fischer, C., Godefroid, M., Brage, T., Jönsson, P., & Gaigalas, G. 2016, *JPhB*, 49, 182004
- Froese Fischer, C., Tachiev, G., & Irimia, A. 2006, *ADNDT*, 92, 607
- Gaigalas, G., Froese Fischer, C., Rynkun, P., & Jönsson, P. 2017, *Atoms*, 5, 6
- Gaigalas, G., Zalandauskas, T., & Fritzsche, S. 2004, *CoPhC*, 157, 239
- Gálvez, F. J., Buendía, E., & Sarsa, A. 2005, *JChPh*, 123, 034302
- Grant, I. P. 1974, *JPhB*, 7, 1458
- Grant, I. P. 2007, *Relativistic Quantum Theory of Atoms and Molecules*, doi:10.1007/978-0-387-35069-1
- Guo, X. L., Huang, M., Yan, J., et al. 2015, *JPhB*, 48, 144020
- Guo, X. L., Si, R., Li, S., et al. 2016, *PhRvA*, 93, 012513
- Gustafsson, S., Jönsson, P., Froese Fischer, C., & Grant, I. 2017, *Atoms*, 5, 3
- Jönsson, P., Gaigalas, G., Bieroń, J., Froese Fischer, C., & Grant, I. P. 2013, *CoPhC*, 184, 2197
- Jönsson, P., He, X., Froese Fischer, C., & Grant, I. 2007, *CoPhC*, 177, 597
- Jönsson, P., Rynkun, P., & Gaigalas, G. 2011, *ADNDT*, 97, 648
- Jönsson, P., Ekman, J., Gustafsson, S., et al. 2013, *A&A*, 559, p. A100
- Jönsson, P., Bengtsson, P., Ekman, J., et al. 2014, *ADNDT*, 100, 1
- Jönsson, P., Gaigalas, G., Rynkun, P., et al. 2017, *Atoms*, 5, 16
- Kramida, A., Yu. Ralchenko, Reader, J., & and NIST ASD Team. 2018, *NIST Atomic Spectra Database (ver. 5.5.2)*, [Online]. Available: <https://physics.nist.gov/asd> [2018, February 21]. National Institute of Standards and Technology, Gaithersburg, MD., ,
- Landi, E., & Bhatia, A. K. 2010, *ADNDT*, 96, 52
- Li, J., Jönsson, P., Dong, C., & Gaigalas, G. 2010, *JPhB*, 43, 035005
- Olsen, J., Godefroid, M. R., Jönsson, P., Malmqvist, P. Å., & Froese Fischer, C. 1995, *PhRvE*, 52, 4499
- Raassen, A. J. J., Mewe, R., Audard, M., et al. 2002, *A&A*, 389, 228
- Si, R., Li, S., Guo, X. L., et al. 2016, *ApJS*, 227, 16
- Si, R., Zhang, C., Liu, Y., et al. 2017, *JQSRT*, 189, 249
- Storey, P. J., Del Zanna, G., Mason, H. E., & Zeppen, C. J. 2005, *A&A*, 433, 717
- Sturesson, L., Jönsson, P., & Froese Fischer, C. 2007, *CoPhC*, 177, 539
- Sugar, J., & Corliss, C. 1985, *JPCRD*, Vol 14, Supplement No 2, 1
- Sugar, J., & Musgrove, A. 1990, *JPCRD*, 19, 527
- . 1995, *JPCRD*, 24, 1803
- Tayal, S. S. 2011, *ADNDT*, 97, 481
- Träbert, E. 1998, *MNRAS*, 297, 399
- Träbert, E., Hoffmann, J., Reinhardt, S., Wolf, A., & Del Zanna, G. 2008, *Journal of Physics: Conference Series*, 130, 012018
- Vilkas, M. J., & Ishikawa, Y. 2004, *JPhB*, 37, 4763
- Wang, K., Jönsson, P., Ekman, J., et al. 2017a, *JQSRT*, 194, 108
- Wang, K., Jnsson, P., Ekman, J., et al. 2017b, *PhRvL*, 119, 189301
- Wang, K., Li, D. F., Liu, H. T., et al. 2014, *ApJS*, 215, 26
- Wang, K., Guo, X. L., Liu, H. T., et al. 2015, *ApJS*, 218, 16
- Wang, K., Si, R., Dang, W., et al. 2016a, *ApJS*, 223, 3
- Wang, K., Chen, Z. B., Si, R., et al. 2016b, *ApJS*, 226, 14
- Wang, K., Li, S., Jönsson, P., et al. 2017c, *JQSRT*, 187, 375
- Wang, K., Jönsson, P., Ekman, J., et al. 2017d, *ApJS*, 229, 37
- Wang, K., Chen, Z. B., Zhang, C. Y., et al. 2018a, *ApJS*, 234, 40
- Wang, K., Zhang, C., Jönsson, P., et al. 2018b, *JQSRT*, 208, 134
- Ynnerman, A., & Fischer, C. F. 1995, *Phys. Rev. A*, 51, 2020
- Young, P. R., Watanabe, T., Hara, H., & Mariska, J. T. 2009, *A&A*, 495, 587
- Zhao, Z., Wang, K., Li, S., et al. 2017, *ADNDT*, 119

**Table 1.** Energy levels (in  $\text{cm}^{-1}$ ) relative to the ground state along with radiative lifetime (in s) for the lowest 143 states of Fe XII.  $E_{CI}$ -the present calculations;  $E_{NIST}$  observed energies listed in the NIST database Kramida et al. (2018);  $E_{CHI1}$  and  $E_{CHI2}$  observed and calculated energies, respectively, listed in the CHIANTI database Dere et al. (1997); Del Zanna et al. (2015);  $E_{MRMP}$  MR-MP calculations by Vilkas & Ishikawa (2004);  $E_{MCHF-BP}$  MCHF-BP calculations by Tayal (2011);  $E_{SS}$  SS calculations by Del Zanna & Mason (2005);  $\tau_{CI}$  lifetimes from the present calculations;  $\tau_{CHI2}$  calculated lifetimes given in the CHIANTI database;  $\tau_{MCHF-BP}$  MCHF-BP calculations by Tayal;  $\tau_{MRMP}$  MR-MP calculations by Vilkas.

Key	Level	$E_{CI}$	$E_{NIST}$	$E_{CHI1}$	$E_{CHI2}$	$E_{MRMP}$	$E_{MCHF-BP}$	$E_{SS}$	$\tau_{CI}$	$\tau_{CHI2}$	$\tau_{MCHF-BP}$	$\tau_{MRMP}$
1	$3s^2 3p^3 (4S) 4S^{\circ}_{3/2}$	0	0	0	0	0	0	0	...	...	...	...
2	$3s^2 3p^3 (2D) 2D^{\circ}_{3/2}$	41771	41566	41555	41556	41518	41567	41555	1.845E-02	2.257E-02	...	...
3	$3s^2 3p^3 (2D) 2D^{\circ}_{5/2}$	46319	46075	46088	46088	46049	45967	46088	3.259E-01	3.808E-01	...	...
4	$3s^2 3p^3 (2P) 2P^{\circ}_{1/2}$	74372	74109	74107	74107	74137	74060	74107	3.845E-03	4.207E-03	...	...
5	$3s^2 3p^3 (2P) 2P^{\circ}_{3/2}$	80762	80515	80515	80515	80536	80481	80515	1.599E-03	1.688E-03	...	...
6	$3s 2S 3p^4 (3P) 4P_{5/2}$	274498	274373	274373	274373	274279	274930	274373	6.118E-10	6.041E-10	6.210E-10	6.750E-10
7	$3s 2S 3p^4 (3P) 4P_{3/2}$	284126	284005	284005	277374	283908	283863	284005	5.659E-10	6.049E-10	5.810E-10	6.250E-10
8	$3s 2S 3p^4 (3P) 4P_{1/2}$	288451	288307	288307	288307	288213	288000	288307	5.355E-10	5.332E-10	5.530E-10	5.920E-10

*Table 1 continued*

Table 1 (continued)

Key	Level	$E_{CI}$	$E_{NIST}$	$E_{CHI1}$	$E_{CHI2}$	$E_{MRMP}$	$E_{MCHF-BP}$	$E_{SS}$	$\tau_{CI}$	$\tau_{CHI2}$	$\tau_{MCHF-BP}$	$\tau_{MRMP}$
9	$3s^2 3p^4(^1D) 2D_{3/2}$	340104	340020	339725	335258	339710	340785	339725	2.717E-10	2.816E-10	2.750E-10	2.990E-10
10	$3s^2 3p^4(^1D) 2D_{5/2}$	342050	341703	341716	341716	341648	342589	341716	3.011E-10	2.958E-10	3.030E-10	3.290E-10
11	$3s^2 3p^4(^3P) 2P_{3/2}$	390073	389706	389719	389719	389767	391084	389719	1.063E-10	1.054E-10	1.050E-10	1.210E-10
12	$3s^2 3p^2(^3P) 3P 3d^2 P_{1/2}$	394712	394120	394360	394360	394282	395860	394360	9.576E-11	9.412E-11	9.530E-11	1.060E-10
13	$3s^2 3p^4(^1S) 2S_{1/2}$	410814	...	410401	410401	409948	411569	410401	1.182E-10	1.142E-10	1.170E-10	1.270E-10
14	$3s^2 3p^2(^3P) 3P 3d^4 F_{3/2}$	427242	...	427034	427034	427100	430901	426920	5.029E-09	5.516E-09	5.770E-09	5.670E-09
15	$3s^2 3p^2(^3P) 3P 3d^4 F_{5/2}$	431014	...	430743	430743	430876	434450	430758	8.827E-09	1.006E-08	1.050E-08	1.020E-08
16	$3s^2 3p^2(^3P) 3P 3d^4 F_{7/2}$	436549	...	436088	436088	436404	439674	436088	3.737E-08	4.464E-08	4.620E-08	4.220E-08
17	$3s^2 3p^2(^1D) 1D 3d^2 F_{5/2}$	443123	...	...	440878	443015	447141	443318	9.499E-09	9.583E-09	9.080E-09	9.060E-09
18	$3s^2 3p^2(^3P) 3P 3d^4 F_{9/2}$	443380	...	443121	440659	443220	446271	443121	9.728E-03	1.035E-02	...	...
19	$3s^2 3p^2(^1D) 1D 3d^2 F_{7/2}$	447412	...	447070	444791	447343	450694	461474	3.065E-08	3.378E-08	3.980E-05	3.440E-08
20	$3s^2 3p^2(^3P) 3P 3d^4 D_{1/2}$	447701	...	...	444138	447679	449717	446977	1.469E-09	1.587E-09	1.630E-09	1.670E-09
21	$3s^2 3p^2(^3P) 3P 3d^4 D_{3/2}$	448757	...	447076	447076	448737	450906	448071	1.438E-09	1.628E-09	1.680E-09	1.680E-09
22	$3s^2 3p^2(^3P) 3P 3d^4 D_{5/2}$	453038	...	452755	452755	452890	455552	451651	2.113E-09	2.625E-09	2.840E-09	2.730E-09
23	$3s^2 3p^2(^3P) 3P 3d^4 D_{7/2}$	462391	...	461474	461474	462180	464848	447070	2.001E-06	1.015E-04	5.540E-06	1.120E-05
24	$3s^2 3p^2(^1D) 1D 3d^2 G_{7/2}$	494743	...	494518	494518	494339	500315	494518	3.685E-09	4.274E-09	4.640E-09	4.250E-09
25	$3s^2 3p^2(^1D) 1D 3d^2 G_{9/2}$	497791	...	497256	497256	497361	503126	497256	4.384E-03	4.630E-03	...	...
26	$3s^2 3p^2(^3P) 3P 3d^2 P_{3/2}$	502205	501800	501800	501800	502033	507797	501800	1.512E-11	1.428E-11	1.410E-11	1.460E-11
27	$3s^2 3p^2(^3P) 3P 3d^4 P_{5/2}$	512757	512510	512508	512508	512785	519325	512508	1.185E-11	1.133E-11	1.100E-11	1.190E-11
28	$3s^2 3p^4(^3P) 2P_{1/2}$	514274	513850	513850	513850	514101	519220	513850	1.498E-11	1.418E-11	1.410E-11	1.440E-11
29	$3s^2 3p^2(^3P) 3P 3d^4 P_{3/2}$	517037	516740	516772	516772	517079	522994	516772	1.173E-11	1.118E-11	1.100E-11	1.170E-11
30	$3s^2 3p^2(^3P) 3P 3d^4 P_{1/2}$	520038	519770	519767	519768	520062	525504	519767	1.121E-11	1.073E-11	1.040E-11	1.120E-11
31	$3s^2 3p^2(^1S) 1S 3d^2 D_{3/2}$	526717	526120	526127	526127	526434	531553	526127	5.603E-11	5.832E-11	5.600E-11	6.200E-11
32	$3s^2 3p^2(^1S) 1S 3d^2 D_{5/2}$	537485	538040	536939	536939	537292	542307	536939	2.900E-11	3.068E-11	3.230E-11	3.370E-11
33	$3s^2 3p^2(^1D) 1D 3d^2 D_{3/2}$	554413	554030	553906	553906	554428	560514	553906	1.395E-11	1.324E-11	1.290E-11	1.350E-11
34	$3s^2 3p^2(^1D) 1D 3d^2 D_{5/2}$	555178	554610	554632	554632	554986	561001	554632	2.163E-11	1.925E-11	1.780E-11	1.920E-11
35	$3s^2 3p^2(^1D) 1D 3d^2 P_{1/2}$	570299	568940	569794	569794	570468	577760	569794	1.475E-11	1.426E-11	1.380E-11	1.510E-11
36	$3s^2 3p^2(^3P) 3P 3d^2 F_{5/2}$	577311	576740	576733	576733	577403	585741	576733	9.607E-12	9.300E-12	9.010E-12	9.700E-12
37	$3s^2 3p^2(^1D) 1D 3d^2 P_{3/2}$	578190	577740	577680	580345	577973	585277	577680	1.434E-11	1.348E-11	1.340E-11	1.440E-11
38	$3s^2 3p^2(^1D) 1D 3d^2 S_{1/2}$	580194	579630	576153	579853	579882	586216	576153	1.475E-11	1.405E-11	1.380E-11	1.440E-11
39	$3s^2 3p^2(^3P) 3P 3d^2 F_{7/2}$	581737	581180	581171	581171	581819	589794	581171	9.613E-12	9.259E-12	9.010E-12	9.700E-12
40	$3s^2 3p^2(^3P) 3P 3d^2 D_{5/2}$	604547	603930	603940	603940	604464	612091	603940	1.071E-11	1.032E-11	1.030E-11	1.080E-11
41	$3s^2 3p^2(^3P) 3P 3d^2 D_{3/2}$	606180	605480	605540	605540	605985	613374	605540	1.098E-11	1.057E-11	1.030E-11	1.430E-11
42	$3s^2 3p^3(^4S) 5S 3d^6 D_{1/2}^o$	626626	...	...	613765	626435	626366	605311	2.404E-08	2.765E-08	2.800E-08	2.650E-08
43	$3s^2 3p^3(^4S) 5S 3d^6 D_{3/2}^o$	626868	...	...	614078	626687	626673	605626	2.612E-08	3.223E-08	3.130E-08	2.960E-08
44	$3s^2 3p^3(^4S) 5S 3d^6 D_{5/2}^o$	627290	...	...	614577	627090	627166	606128	3.673E-08	4.630E-08	4.560E-08	4.060E-08
45	$3s^2 3p^3(^4S) 5S 3d^6 D_{7/2}^o$	627861	...	...	615273	627663	627853	606827	7.206E-08	9.611E-08	9.680E-08	8.280E-08
46	$3s^2 3p^3(^4S) 5S 3d^6 D_{9/2}^o$	628724	...	...	616260	628538	628828	607820	9.355E-08	1.145E-07	1.130E-07	1.130E-07
47	$3p^5 2P_{3/2}^o$	636770	...	...	627294	...	637541	616074	1.290E-10	1.360E-10	1.260E-10	...
48	$3p^5 2P_{1/2}^o$	651603	...	...	641642	...	651329	630899	1.319E-10	1.359E-10	1.290E-10	...
49	$3s^2 3p^3(^2D) 3D 3d^4 D_{5/2}^o$	680968	...	...	671063	...	683778	662950	1.666E-09	1.839E-09	1.810E-09	...
50	$3s^2 3p^3(^2D) 3D 3d^4 D_{7/2}^o$	681593	...	...	671652	...	684317	663573	2.340E-09	2.508E-09	2.460E-09	...
51	$3s^2 3p^3(^2D) 3D 3d^4 D_{3/2}^o$	681939	...	...	671969	...	684669	663879	1.557E-09	1.726E-09	1.720E-09	...
52	$3s^2 3p^3(^2D) 3D 3d^4 D_{1/2}^o$	683673	...	...	673495	...	686116	665514	1.842E-09	2.001E-09	1.980E-09	...
53	$3s^2 3p^3(^2D) 3D 3d^4 F_{3/2}^o$	690715	...	...	681077	...	693867	672503	7.336E-10	7.622E-10	7.330E-10	...
54	$3s^2 3p^3(^2D) 3D 3d^4 F_{5/2}^o$	693007	...	...	683420	...	696044	674873	7.504E-10	7.844E-10	7.520E-10	...
55	$3s^2 3p^3(^2D) 3D 3d^4 F_{7/2}^o$	695830	...	...	686355	...	698790	677823	7.680E-10	8.027E-10	7.700E-10	...
56	$3s^2 3p^3(^2D) 3D 3d^4 F_{9/2}^o$	699589	...	...	690188	...	702435	681683	8.049E-10	8.211E-10	8.050E-10	...
57	$3s^2 3p^3(^2D) 3D 3d^2 S_{1/2}^o$	723741	...	...	715091	...	727016	707089	3.806E-10	3.898E-10	3.680E-10	...
58	$3s^2 3p^3(^2D) 3D 3d^4 G_{5/2}^o$	728057	...	...	721201	...	731775	713668	2.566E-10	2.593E-10	2.570E-10	...
59	$3s^2 3p^3(^2D) 3D 3d^4 G_{7/2}^o$	729029	...	...	722212	...	732757	714678	2.630E-10	2.656E-10	2.630E-10	...
60	$3s^2 3p^3(^2D) 3D 3d^4 G_{9/2}^o$	730383	...	...	723629	...	734111	716086	2.734E-10	2.747E-10	2.730E-10	...
61	$3s^2 3p^3(^2D) 3D 3d^4 G_{11/2}^o$	732384	...	...	725569	...	735910	718003	2.883E-10	2.830E-10	2.870E-10	...
62	$3s^2 3p^3(^2D) 3D 3d^2 G_{7/2}^o$	756749	...	...	751470	...	761329	743686	5.188E-10	5.213E-10	5.280E-10	...
63	$3s^2 3p^3(^2D) 3D 3d^2 G_{9/2}^o$	756809	...	...	751570	...	761239	743824	4.877E-10	4.847E-10	4.970E-10	...
64	$3s^2 3p^3(^2P) 3P 3d^4 D_{1/2}^o$	760728	...	...	753742	...	766760	749249	1.287E-10	1.288E-10	1.260E-10	...
65	$3s^2 3p^3(^2P) 3P 3d^4 D_{3/2}^o$	762125	...	...	754888	...	767794	747455	9.250E-11	8.593E-11	8.680E-11	...

Table 1 continued



Table 1 (continued)

Key	Level	$E_{CI}$	$E_{NIST}$	$E_{CHI1}$	$E_{CHI2}$	$E_{MRMP}$	$E_{MCHF-BP}$	$E_{SS}$	$\tau_{CI}$	$\tau_{CHI2}$	$\tau_{MCHF-BP}$	$\tau_{MRMP}$
66	$3s^2 S 3p^3(2P) 3P 3d^4 D_{5/2}^{\circ}$	763921	...	...	756775	...	769490	749158	6.016E-11	5.232E-11	5.780E-11	...
67	$3s^2 S 3p^3(2P) 3P 3d^4 P_{1/2}^{\circ}$	764825	...	...	756687	...	769582	746760	1.757E-10	1.611E-10	1.660E-10	...
68	$3s^2 S 3p^3(2P) 3P 3d^4 P_{3/2}^{\circ}$	766070	...	...	758580	...	771465	751398	9.336E-11	1.006E-10	9.790E-11	...
69	$3s^2 S 3p^3(2P) 3P 3d^4 F_{5/2}^{\circ}$	771203	...	...	763630	...	776463	756314	4.498E-11	5.154E-11	4.560E-11	...
70	$3s^2 S 3p^3(2P) 3P 3d^2 D_{3/2}^{\circ}$	772021	...	...	765853	...	777348	758205	1.253E-10	1.293E-10	1.260E-10	...
71	$3s^2 S 3p^3(2P) 3P 3d^2 D_{5/2}^{\circ}$	773320	...	...	766983	...	778955	759741	8.827E-11	8.595E-11	8.920E-11	...
72	$3s^2 S 3p^3(4S) 5S 3d^4 D_{7/2}^{\circ}$	775583	...	...	768699	...	781096	761930	1.250E-10	1.190E-10	1.180E-10	...
73	$3s^2 S 3p^3(2P) 3P 3d^4 F_{9/2}^{\circ}$	777121	...	...	771432	...	782418	764134	1.227E-10	1.177E-10	1.170E-10	...
74	$3s^2 S 3p^3(2P) 3P 3d^4 F_{7/2}^{\circ}$	778390	...	...	772442	...	783801	765403	9.173E-11	9.430E-11	9.170E-11	...
75	$3s^2 S 3p^3(2P) 3P 3d^4 F_{5/2}^{\circ}$	779213	...	...	773364	...	784684	766306	9.865E-11	9.748E-11	9.710E-11	...
76	$3s^2 S 3p^3(2P) 3P 3d^4 F_{3/2}^{\circ}$	780241	...	...	774317	...	785709	767311	1.034E-10	1.006E-10	1.000E-10	...
77	$3s^2 S 3p^3(2D) 3D 3d^4 S_{3/2}^{\circ}$	788073	...	...	781907	...	793590	778031	1.733E-11	1.475E-11	1.570E-11	...
78	$3s^2 S 3p^3(2D) 3D 3d^4 P_{5/2}^{\circ}$	789866	...	...	782831	...	795165	776267	1.978E-11	1.832E-11	1.720E-11	...
79	$3s^2 S 3p^3(2D) 3D 3d^4 P_{3/2}^{\circ}$	790861	...	...	784839	...	796690	775232	1.326E-11	1.436E-11	1.270E-11	...
80	$3s^2 S 3p^3(2D) 1D 3d^2 F_{7/2}^{\circ}$	792345	...	...	787182	...	798425	779422	1.422E-10	1.442E-10	1.410E-10	...
81	$3s^2 S 3p^3(2D) 1D 3d^2 F_{5/2}^{\circ}$	792950	...	...	787732	...	798649	780009	7.607E-11	9.339E-11	8.510E-11	...
82	$3s^2 S 3p^3(2D) 3D 3d^4 P_{1/2}^{\circ}$	793069	...	...	785515	...	798356	778670	1.183E-11	1.146E-11	1.110E-11	...
83	$3s^2 S 3p^3(2D) 1D 3d^2 D_{5/2}^{\circ}$	807707	...	...	803238	...	813626	795699	3.438E-11	3.224E-11	3.500E-11	...
84	$3s^2 S 3p^3(2P) 3P 3d^4 D_{7/2}^{\circ}$	810021	...	800578	804964	...	817360	797914	1.323E-11	1.287E-11	1.260E-11	...
85	$3s^2 S 3p^3(2D) 3D 3d^2 D_{3/2}^{\circ}$	810227	...	805335	805335	...	816115	798679	3.897E-11	3.752E-11	3.700E-11	...
86	$3s^2 S 3p^3(4S) 5S 3d^4 D_{1/2}^{\circ}$	813443	...	...	808143	...	820581	800951	1.429E-11	1.389E-11	1.350E-11	...
87	$3s^2 S 3p^3(4S) 5S 3d^4 D_{5/2}^{\circ}$	813759	...	804375	808588	...	820798	801592	1.413E-11	1.364E-11	1.300E-11	...
88	$3s^2 S 3p^3(4S) 5S 3d^4 D_{3/2}^{\circ}$	814618	...	...	809384	...	821697	802397	1.332E-11	1.292E-11	1.270E-11	...
89	$3s^2 S 3p^3(2D) 3D 3d^2 P_{1/2}^{\circ}$	820046	...	...	814316	...	826827	807026	1.310E-11	1.271E-11	1.240E-11	...
90	$3s^2 S 3p^3(2D) 3D 3d^2 P_{3/2}^{\circ}$	820056	...	...	814397	...	827068	806881	1.329E-11	1.307E-11	1.240E-11	...
91	$3s^2 S 3p^3(2D) 1D 3d^2 G_{7/2}^{\circ}$	823509	...	...	820798	...	830645	813738	4.593E-11	4.662E-11	4.490E-11	...
92	$3s^2 S 3p^3(2P) 3P 3d^2 F_{5/2}^{\circ}$	827269	...	...	823124	...	834929	816285	8.674E-11	8.128E-11	8.460E-11	...
93	$3s^2 S 3p^3(2D) 1D 3d^2 G_{9/2}^{\circ}$	831086	...	...	829548	...	837888	822255	5.053E-11	4.738E-11	4.820E-11	...
94	$3s^2 S 3p^3(2P) 3P 3d^2 F_{7/2}^{\circ}$	833600	...	...	830864	...	840453	823768	5.786E-11	5.321E-11	5.710E-11	...
95	$3s^2 S 3p^3(4S) 3S 3d^4 D_{3/2}^{\circ}$	857471	...	...	855285	...	865754	848276	1.466E-11	1.404E-11	1.360E-11	...
96	$3s^2 S 3p^3(4S) 3S 3d^4 D_{5/2}^{\circ}$	857686	...	...	855716	...	865896	848510	1.401E-11	1.333E-11	1.310E-11	...
97	$3s^2 S 3p^3(4S) 3S 3d^4 D_{7/2}^{\circ}$	858047	...	...	856214	...	866146	848931	1.466E-11	1.376E-11	1.370E-11	...
98	$3s^2 S 3p^3(4S) 3S 3d^4 D_{1/2}^{\circ}$	858979	...	...	856605	...	867067	849567	1.384E-11	1.341E-11	1.280E-11	...
99	$3s^2 S 3p^3(2D) 1D 3d^2 D_{3/2}^{\circ}$	862239	...	...	860018	...	870586	853261	1.636E-11	1.543E-11	1.570E-11	...
100	$3s^2 S 3p^3(2D) 3D 3d^2 D_{5/2}^{\circ}$	867231	...	...	864831	...	875488	858210	1.634E-11	1.571E-11	1.570E-11	...
101	$3s^2 S 3p^3(2P) 3P 3d^2 P_{1/2}^{\circ}$	870038	...	...	866782	...	878856	859991	2.289E-11	2.168E-11	2.230E-11	...
102	$3s^2 S 3p^3(2D) 3D 3d^2 F_{5/2}^{\circ}$	871192	...	...	869129	...	880366	862455	1.640E-11	1.524E-11	1.550E-11	...
103	$3s^2 S 3p^3(2D) 3D 3d^2 F_{7/2}^{\circ}$	875985	...	...	873492	...	884748	866839	1.411E-11	1.367E-11	1.350E-11	...
104	$3s^2 S 3p^3(2P) 3P 3d^2 P_{3/2}^{\circ}$	879252	...	...	875782	...	887637	869164	3.090E-11	2.885E-11	2.900E-11	...
105	$3s^2 3p^2 P 3d^2(3F) 4G_{5/2}^{\circ}$	884704	...	...	884958	...	894124	876786	4.047E-11	3.984E-11	3.870E-11	...
106	$3s^2 3p^2 P 3d^2(3F) 4G_{7/2}^{\circ}$	887850	...	...	888150	...	897162	879950	4.425E-11	4.343E-11	4.240E-11	...
107	$3s^2 S 3p^3(2P) 1P 3d^2 D_{3/2}^{\circ}$	890406	...	...	889593	...	900248	881781	1.642E-11	1.529E-11	1.530E-11	...
108	$3s^2 3p^2 P 3d^2(3F) 4G_{9/2}^{\circ}$	892596	...	...	892834	...	901671	884693	5.117E-11	4.798E-11	4.810E-11	...
109	$3s^2 3p^2 P 3d^2(3P) 2S_{1/2}^{\circ}$	892670	...	...	892154	...	901919	886838	1.271E-11	1.198E-11	1.190E-11	...
110	$3s^2 S 3p^3(2P) 1P 3d^2 D_{5/2}^{\circ}$	894591	...	...	894046	...	904359	886467	1.705E-11	1.619E-11	1.600E-11	...
111	$3s^2 3p^2 P 3d^2(3F) 4G_{11/2}^{\circ}$	899639	...	...	899389	...	908094	891480	5.247E-11	4.851E-11	4.920E-11	...
112	$3s^2 S 3p^3(2P) 1P 3d^2 F_{5/2}^{\circ}$	901175	...	...	901637	...	911473	895165	1.520E-11	1.416E-11	1.410E-11	...
113	$3s^2 3p^2 P 3d^2(1D) 2P_{3/2}^{\circ}$	901708	...	...	901218	...	912848	894223	9.648E-12	9.260E-12	8.950E-12	...
114	$3s^2 S 3p^3(2P) 1P 3d^2 F_{7/2}^{\circ}$	902442	...	...	903141	...	912659	896879	1.568E-11	1.482E-11	1.470E-11	...
115	$3s^2 3p^2 P 3d^2(1D) 2P_{1/2}^{\circ}$	912069	...	...	911281	...	922408	904421	9.780E-12	9.384E-12	9.040E-12	...
116	$3s^2 3p^2 P 3d^2(3P) 4D_{1/2}^{\circ}$	933511	...	...	933978	...	945584	926095	1.943E-11	1.808E-11	1.830E-11	...
117	$3s^2 3p^2 P 3d^2(3P) 4D_{3/2}^{\circ}$	935076	...	...	935697	...	947219	927883	1.954E-11	1.819E-11	1.840E-11	...
118	$3s^2 3p^2 P 3d^2(3P) 4D_{5/2}^{\circ}$	937497	...	...	938432	...	949609	930733	1.852E-11	1.769E-11	1.760E-11	...
119	$3s^2 3p^2 P 3d^2(3P) 4D_{7/2}^{\circ}$	942750	...	...	943564	...	954544	935897	1.829E-11	1.735E-11	1.760E-11	...
120	$3s^2 3p^2 P 3d^2(1D) 2F_{5/2}^{\circ}$	943795	...	...	946333	...	955980	938856	1.540E-11	1.416E-11	1.450E-11	...

Table 1 continued

Table 1 (continued)

Key	Level	$E_{CI}$	$E_{NIST}$	$E_{CHI1}$	$E_{CHI2}$	$E_{MRMP}$	$E_{MCHF-BP}$	$E_{SS}$	$\tau_{CI}$	$\tau_{CHI2}$	$\tau_{MCHF-BP}$	$\tau_{MRMP}$
121	$3s^2 2S 3p^3(2P) 1P 3d^2 2F_{3/2}^o$	946196	...	...	947923	...	958447	942424	1.001E-11	9.417E-12	9.710E-12	...
122	$3s^2 2S 3p^3(2P) 1P 3d^2 2P_{1/2}^o$	947486	...	...	948891	...	959236	904421	1.027E-11	9.619E-12	9.580E-12	...
123	$3s^2 3p^2 2P 3d^2(3F) 4F_{3/2}^o$	949240	...	...	950416	...	966517	947260	1.050E-11	9.984E-12	1.480E-11	...
124	$3s^2 3p^2 2P 3d^2(3P) 4F_{1/2}^o$	951071	...	...	951340	...	963223	943706	1.570E-11	1.461E-11	1.480E-11	...
125	$3s^2 3p^2 2P 3d^2(1G) 2H_{9/2}^o$	951338	...	...	955124	...	969677	950047	3.478E-11	2.700E-11	1.000E-11	...
126	$3s^2 3p^2 2P 3d^2(3F) 4F_{5/2}^o$	951419	...	...	952569	...	971163	952879	1.065E-11	1.013E-11	1.340E-11	...
127	$3s^2 3p^2 2P 3d^2(1D) 2F_{7/2}^o$	953092	...	...	954959	...	964994	896879	1.544E-11	1.227E-11	1.460E-11	...
128	$3s^2 3p^2 2P 3d^2(3F) 4F_{7/2}^o$	954273	...	...	955735	...	968063	947779	1.108E-11	1.183E-11	9.990E-12	...
129	$3s^2 3p^2 2P 3d^2(3P) 4F_{3/2}^o$	954662	...	...	954800	...	963356	943041	1.566E-11	1.464E-11	9.650E-12	...
130	$3s^2 3p^2 2P 3d^2(3F) 4F_{9/2}^o$	955740	...	...	957386	...	975476	946809	1.120E-11	1.127E-11	2.940E-11	...
131	$3s^2 3p^2 2P 3d^2(3P) 4F_{5/2}^o$	959371	...	...	959981	...	965428	945234	1.340E-11	1.387E-11	9.750E-12	...
132	$3s^2 3p^2 2P 3d^2(1D) 2D_{3/2}^o$	961709	...	...	964696	...	973880	959673	1.287E-11	1.195E-11	1.220E-11	...
133	$3s^2 3p^2 2P 3d^2(3F) 2D_{5/2}^o$	962689	...	...	965102	...	974987	959886	1.237E-11	1.057E-11	1.130E-11	...
134	$3s^2 3p^2 2P 3d^2(1G) 2H_{11/2}^o$	965831	...	...	968595	...	989184	960769	3.905E-11	3.634E-11	3.490E-11	...
135	$3s^2 3p^2 2P 3d^2(1G) 2G_{7/2}^o$	973479	...	...	976467	...	986346	968843	1.318E-11	1.238E-11	1.240E-11	...
136	$3s^2 3p^2 2P 3d^2(1G) 2G_{9/2}^o$	977416	...	...	980179	...	988863	972709	1.351E-11	1.271E-11	1.230E-11	...
137	$3s^2 2S 3p^3(4S) 3S 3d^2 2D_{5/2}^o$	985879	...	...	989265	...	999134	984050	8.257E-12	7.707E-12	8.010E-12	...
138	$3s^2 2S 3p^3(4S) 3S 3d^2 2D_{3/2}^o$	988395	...	...	991715	...	1001920	986385	7.496E-12	7.035E-12	7.340E-12	...
139	$3s^2 3p^2 2P 3d^2(3F) 4D_{5/2}^o$	993058	...	...	996707	...	1006724	989745	8.173E-12	7.619E-12	7.600E-12	...
140	$3s^2 3p^2 2P 3d^2(3F) 4D_{3/2}^o$	994346	...	...	997781	...	1007748	990850	8.121E-12	7.600E-12	7.560E-12	...
141	$3s^2 3p^2 2P 3d^2(3F) 4D_{3/2}^o$	995533	...	...	998815	...	1008725	991932	8.037E-12	7.529E-12	7.470E-12	...
142	$3s^2 3p^2 2P 3d^2(3F) 4D_{1/2}^o$	996341	...	...	999367	...	1009349	992666	7.914E-12	7.280E-12	7.390E-12	...
143	$3s^2 2S 3p^3(2D) 1D 3d^2 2S_{1/2}^o$	997100	...	...	999866	...	1010157	993536	7.668E-12	7.278E-12	7.120E-12	...

**Table 2.** Mean level deviation  $MLD$  and energy shift  $ES$  (in  $\text{cm}^{-1}$ ) for the MCDHF/CI and MRMP calculations obtained from Eq. 4.

$Z$	MCDHF/CI		MR-MP	
	$ES$	$MLD$	$ES$	$MLD$
24	333	151	...	...
25	383	144	...	...
26	367	213	233	271
27	326	139	47	216
28	345	122	68	182
29	385	206	72	232
30	280	146	66	202

**Table 3.** Energy levels (in  $\text{cm}^{-1}$ ) relative to the ground state along with radiative lifetime (in s) for the lowest 143 states of Cr X, Mn XI, Fe XII, Co XIII, Ni XIV, Cu XV, Zn XVI.  $E_{CI1}$  the present *ab initio* calculations;  $E_{CI2}$  the present calculations where energies of excited states have been shifted by a constant  $ES$  given in Table 2 (see text for more details).  $E_{NIST}$  observed energies listed in the NIST database [Kramida et al. \(2018\)](#);  $E_{MRMP}$  MRMP calculations by [Vilkas & Ishikawa \(2004\)](#);  $\tau_1$  lifetimes in s from the present calculations in length gauge;  $\tau_v$  lifetimes from the present calculations in velocity gauge.

$Z$	Key	Level	$E_{CI1}$	$E_{CI2}$	$E_{NIST}$	$E_{MRMP}$	$\tau_1$	$\tau_v$
28	1	$3s^2 3p^3(4S) 4S_{3/2}^o$	0	0	0	0	...	...
28	2	$3s^2 3p^3(2D) 2D_{3/2}^o$	45978	45633	45767	45729	5.502E-03	...

Table 3 continued

Table 3 (continued)

Z	Key	Level	$E_{CI1}$	$E_{CI2}$	$E_{NIST}$	$E_{MRMP}$	$\tau_1$	$\tau_v$
28	3	$3s^2 3p^3(2D) 2D_{5/2}^{\circ}$	53798	53453	53569	53534	7.165E-02	...
28	4	$3s^2 3p^3(2P) 2P_{1/2}^{\circ}$	85396	85051	85126	85151	1.513E-03	...
28	5	$3s^2 3p^3(2P) 2P_{3/2}^{\circ}$	96909	96564	96630	96678	6.313E-04	...
28	6	$3s^2 S 3p^4(3P) 4P_{5/2}$	316478	316133	316343	316237	4.768E-10	4.631E-10
28	7	$3s^2 S 3p^4(3P) 4P_{3/2}$	330975	330630	330837	330739	4.291E-10	4.208E-10
28	8	$3s^2 S 3p^4(3P) 4P_{1/2}$	336908	336563	...	336644	3.988E-10	3.924E-10
28	9	$3s^2 S 3p^4(1D) 2D_{3/2}$	392288	391943	391916	391876	2.058E-10	2.019E-10
28	10	$3s^2 S 3p^4(1D) 2D_{5/2}$	395915	395570	395567	395492	2.367E-10	2.311E-10
28	11	$3s^2 S 3p^4(3P) 2P_{3/2}$	448151	447806	447765	447833	8.714E-11	8.590E-11
28	12	$3s^2 S 3p^4(3P) 2P_{1/2}$	453274	452929	452850	452759	7.482E-11	7.389E-11
28	13	$3s^2 S 3p^4(1S) 2S_{1/2}$	476429	476084	...	475600	9.822E-11	9.696E-11
28	14	$3s^2 3p^2(3P) 3P 3d 4F_{3/2}$	485668	485323	...	485518	2.187E-09	2.159E-09
28	15	$3s^2 3p^2(3P) 3P 3d 4F_{5/2}$	491480	491135	...	491339	3.886E-09	3.899E-09
28	16	$3s^2 3p^2(3P) 3P 3d 4F_{7/2}$	500093	499748	...	499953	2.183E-08	2.267E-08
28	17	$3s^2 3p^2(1D) 1D 3d 2F_{5/2}$	505257	504912	...	505112	4.676E-09	4.709E-09
28	18	$3s^2 3p^2(3P) 3P 3d 4F_{9/2}$	510176	509831	...	510020	6.386E-03	1.415E-02
28	19	$3s^2 3p^2(1D) 1D 3d 2F_{7/2}$	511825	511480	...	511727	1.859E-08	1.926E-08
28	20	$3s^2 3p^2(3P) 3P 3d 4D_{1/2}$	512200	511855	...	512170	6.805E-10	6.728E-10
28	21	$3s^2 3p^2(3P) 3P 3d 4D_{3/2}$	513581	513236	...	513554	6.835E-10	6.789E-10
28	22	$3s^2 3p^2(3P) 3P 3d 4D_{5/2}$	520172	519827	...	520055	1.004E-09	1.009E-09
28	23	$3s^2 3p^2(3P) 3P 3d 4D_{7/2}$	534358	534013	...	534182	1.515E-07	1.531E-07
28	24	$3s^2 3p^2(1D) 1D 3d 2G_{7/2}$	566449	566104	...	566059	1.764E-09	1.778E-09
28	25	$3s^2 3p^2(1D) 1D 3d 2G_{9/2}$	571637	571292	...	571224	1.809E-03	2.466E-02
28	26	$3s^2 3p^2(3P) 3P 3d 2P_{3/2}$	572152	571807	...	571956	1.270E-11	1.264E-11
28	27	$3s^2 3p^2(3P) 3P 3d 4P_{5/2}$	583763	583418	583530	583742	1.033E-11	1.036E-11
28	28	$3s^2 3p^2(3P) 3P 3d 2P_{1/2}$	589420	589075	...	589258	1.209E-11	1.206E-11
28	29	$3s^2 3p^2(3P) 3P 3d 4P_{3/2}$	589584	589239	589310	589571	1.039E-11	1.041E-11
28	30	$3s^2 3p^2(3P) 3P 3d 4P_{1/2}$	594994	594649	594810	594928	9.934E-12	9.931E-12
28	31	$3s^2 3p^2(1S) 1S 3d 2D_{3/2}$	601140	600795	...	600866	4.306E-11	4.315E-11
28	32	$3s^2 3p^2(1S) 1S 3d 2D_{5/2}$	616153	615808	...	615994	1.987E-11	1.989E-11
28	33	$3s^2 3p^2(1D) 1D 3d 2D_{3/2}$	632735	632390	632280	632733	1.167E-11	1.167E-11
28	34	$3s^2 3p^2(1D) 1D 3d 2D_{5/2}$	635023	634678	634430	634755	2.317E-11	2.318E-11
28	35	$3s^2 3p^2(1D) 1D 3d 2P_{1/2}$	648863	648518	648320	648835	1.291E-11	1.295E-11
28	36	$3s^2 3p^2(3P) 3P 3d 2F_{5/2}$	655365	655020	...	655416	8.404E-12	8.434E-12
28	37	$3s^2 3p^2(1D) 1D 3d 2P_{3/2}$	661229	660884	660710	660991	1.244E-11	1.249E-11
28	38	$3s^2 3p^2(3P) 3P 3d 2F_{7/2}$	663125	662780	662780	663166	8.433E-12	8.467E-12
28	39	$3s^2 3p^2(1D) 1D 3d 2S_{1/2}$	663638	663293	...	663497	1.247E-11	1.247E-11
28	40	$3s^2 3p^2(3P) 3P 3d 2D_{5/2}$	691152	690807	690560	691050	9.378E-12	9.416E-12
28	41	$3s^2 3p^2(3P) 3P 3d 2D_{3/2}$	692453	692108	691930	692203	9.694E-12	9.734E-12
28	42	$3s^2 S 3p^3(4S) 5S 3d 6D_{1/2}^{\circ}$	722107	721762	...	721955	1.206E-08	1.168E-08
28	43	$3s^2 S 3p^3(4S) 5S 3d 6D_{3/2}^{\circ}$	722506	722161	...	722362	1.215E-08	1.183E-08
28	44	$3s^2 S 3p^3(4S) 5S 3d 6D_{5/2}^{\circ}$	723163	722818	...	723000	1.688E-08	1.659E-08
28	45	$3s^2 S 3p^3(4S) 5S 3d 6D_{7/2}^{\circ}$	724067	723722	...	723908	3.247E-08	3.194E-08
28	46	$3s^2 S 3p^3(4S) 5S 3d 6D_{9/2}^{\circ}$	725575	725230	...	725410	4.099E-08	3.780E-08
28	47	$3p^5 2P_{3/2}^{\circ}$	732838	732493	...	...	1.009E-10	9.934E-11
28	48	$3p^5 2P_{1/2}^{\circ}$	754885	754540	...	...	1.042E-10	1.028E-10
28	49	$3s^2 S 3p^3(2D) 3D 3d 4D_{5/2}^{\circ}$	782853	782508	...	...	1.081E-09	1.053E-09
28	50	$3s^2 S 3p^3(2D) 3D 3d 4D_{3/2}^{\circ}$	784172	783827	...	...	9.509E-10	9.305E-10
28	51	$3s^2 S 3p^3(2D) 3D 3d 4D_{7/2}^{\circ}$	784603	784258	...	...	1.727E-09	1.664E-09
28	52	$3s^2 S 3p^3(2D) 3D 3d 4D_{1/2}^{\circ}$	787752	787407	...	...	1.318E-09	1.296E-09
28	53	$3s^2 S 3p^3(2D) 3D 3d 4F_{3/2}^{\circ}$	793933	793588	...	...	5.835E-10	5.715E-10
28	54	$3s^2 S 3p^3(2D) 3D 3d 4F_{5/2}^{\circ}$	797187	796842	...	...	5.780E-10	5.653E-10
28	55	$3s^2 S 3p^3(2D) 3D 3d 4F_{7/2}^{\circ}$	801241	800896	...	...	5.872E-10	5.730E-10
28	56	$3s^2 S 3p^3(2D) 3D 3d 4F_{9/2}^{\circ}$	806904	806559	...	...	6.189E-10	6.015E-10
28	57	$3s^2 S 3p^3(2D) 3D 3d 2S_{1/2}^{\circ}$	831875	831530	...	...	2.907E-10	2.858E-10
28	58	$3s^2 S 3p^3(2D) 3D 3d 4G_{5/2}^{\circ}$	836142	835797	...	...	1.936E-10	1.908E-10
28	59	$3s^2 S 3p^3(2D) 3D 3d 4G_{7/2}^{\circ}$	837754	837409	...	...	1.999E-10	1.966E-10

Table 3 continued

Table 3 (continued)

Z	Key	Level	$E_{CI1}$	$E_{CI2}$	$E_{NIST}$	$E_{MRMP}$	$\tau_1$	$\tau_v$
28	60	$3s^2 S 3p^3 ({}^2D) {}^3D 3d^4 G_{9/2}^{\circ}$	840052	839707	...	...	2.108E-10	2.069E-10
28	61	$3s^2 S 3p^3 ({}^2D) {}^3D 3d^4 G_{11/2}^{\circ}$	843307	842962	...	...	2.268E-10	2.215E-10
28	62	$3s^2 S 3p^3 ({}^2D) {}^3D 3d^2 G_{7/2}^{\circ}$	868547	868202	...	...	3.751E-10	3.690E-10
28	63	$3s^2 S 3p^3 ({}^2D) {}^3D 3d^2 G_{9/2}^{\circ}$	868900	868555	...	...	3.452E-10	3.373E-10
28	64	$3s^2 S 3p^3 ({}^2P) {}^3P 3d^4 D_{1/2}^{\circ}$	870370	870025	...	...	1.020E-10	1.017E-10
28	65	$3s^2 S 3p^3 ({}^2P) {}^3P 3d^4 D_{3/2}^{\circ}$	872720	872375	...	...	7.329E-11	7.318E-11
28	66	$3s^2 S 3p^3 ({}^4S) {}^5S 3d^4 D_{5/2}^{\circ}$	874978	874633	...	...	4.719E-11	4.722E-11
28	67	$3s^2 S 3p^3 ({}^2P) {}^3P 3d^4 P_{1/2}^{\circ}$	877789	877444	...	...	1.627E-10	1.612E-10
28	68	$3s^2 S 3p^3 ({}^2P) {}^3P 3d^4 P_{3/2}^{\circ}$	878652	878307	...	...	7.164E-11	7.170E-11
28	69	$3s^2 S 3p^3 ({}^2P) {}^3P 3d^4 P_{5/2}^{\circ}$	885854	885509	...	...	2.577E-11	2.582E-11
28	70	$3s^2 S 3p^3 ({}^2P) {}^3P 3d^2 D_{3/2}^{\circ}$	886755	886410	...	...	9.010E-11	8.979E-11
28	71	$3s^2 S 3p^3 ({}^2P) {}^3P 3d^2 D_{5/2}^{\circ}$	888294	887949	...	...	9.928E-11	9.890E-11
28	72	$3s^2 S 3p^3 ({}^4S) {}^5S 3d^4 D_{7/2}^{\circ}$	892202	891857	...	...	1.017E-10	1.010E-10
28	73	$3s^2 S 3p^3 ({}^2P) {}^3P 3d^4 F_{9/2}^{\circ}$	893922	893577	...	...	1.015E-10	1.004E-10
28	74	$3s^2 S 3p^3 ({}^2P) {}^3P 3d^4 F_{7/2}^{\circ}$	894975	894630	...	...	6.125E-11	6.115E-11
28	75	$3s^2 S 3p^3 ({}^2P) {}^3P 3d^4 F_{5/2}^{\circ}$	895791	895446	...	...	7.333E-11	7.288E-11
28	76	$3s^2 S 3p^3 ({}^2P) {}^3P 3d^4 F_{3/2}^{\circ}$	897353	897008	...	...	7.861E-11	7.806E-11
28	77	$3s^2 S 3p^3 ({}^2D) {}^3D 3d^4 F_{3/2}^{\circ}$	904193	903848	...	...	1.454E-11	1.461E-11
28	78	$3s^2 S 3p^3 ({}^2D) {}^3D 3d^4 P_{5/2}^{\circ}$	906835	906490	...	...	2.135E-11	2.138E-11
28	79	$3s^2 S 3p^3 ({}^2D) {}^3D 3d^4 S_{3/2}^{\circ}$	908010	907665	...	...	1.204E-11	1.211E-11
28	80	$3s^2 S 3p^3 ({}^2D) {}^1D 3d^2 F_{7/2}^{\circ}$	909373	909028	...	...	1.038E-10	1.030E-10
28	81	$3s^2 S 3p^3 ({}^2D) {}^3D 3d^4 P_{1/2}^{\circ}$	910973	910628	...	...	1.004E-11	1.007E-11
28	82	$3s^2 S 3p^3 ({}^2D) {}^1D 3d^2 F_{5/2}^{\circ}$	911275	910930	...	...	4.986E-11	4.972E-11
28	83	$3s^2 S 3p^3 ({}^2D) {}^1D 3d^2 D_{5/2}^{\circ}$	925860	925515	...	...	2.383E-11	2.382E-11
28	84	$3s^2 S 3p^3 ({}^2P) {}^3P 3d^4 D_{7/2}^{\circ}$	927488	927143	...	...	1.199E-11	1.205E-11
28	85	$3s^2 S 3p^3 ({}^2D) {}^3D 3d^2 D_{3/2}^{\circ}$	929673	929328	...	...	3.154E-11	3.144E-11
28	86	$3s^2 S 3p^3 ({}^4S) {}^5S 3d^4 D_{1/2}^{\circ}$	930820	930475	...	...	1.274E-11	1.277E-11
28	87	$3s^2 S 3p^3 ({}^2P) {}^3P 3d^4 D_{5/2}^{\circ}$	933150	932805	...	...	1.400E-11	1.405E-11
28	88	$3s^2 S 3p^3 ({}^4S) {}^5S 3d^4 D_{3/2}^{\circ}$	933310	932965	...	...	1.188E-11	1.192E-11
28	89	$3s^2 S 3p^3 ({}^2D) {}^3D 3d^2 F_{3/2}^{\circ}$	940601	940256	...	...	1.123E-11	1.124E-11
28	90	$3s^2 S 3p^3 ({}^2D) {}^3D 3d^2 P_{1/2}^{\circ}$	941071	940726	...	...	1.114E-11	1.116E-11
28	91	$3s^2 S 3p^3 ({}^2D) {}^1D 3d^2 G_{7/2}^{\circ}$	943912	943567	...	...	3.529E-11	3.511E-11
28	92	$3s^2 S 3p^3 ({}^2P) {}^3P 3d^2 F_{5/2}^{\circ}$	949535	949190	...	...	7.119E-11	7.103E-11
28	93	$3s^2 S 3p^3 ({}^2D) {}^1D 3d^2 G_{9/2}^{\circ}$	954897	954552	...	...	4.057E-11	4.016E-11
28	94	$3s^2 S 3p^3 ({}^2P) {}^3P 3d^2 F_{7/2}^{\circ}$	958341	957996	...	...	4.444E-11	4.421E-11
28	95	$3s^2 S 3p^3 ({}^4S) {}^3S 3d^4 D_{3/2}^{\circ}$	981033	980688	...	...	1.235E-11	1.234E-11
28	96	$3s^2 S 3p^3 ({}^4S) {}^3S 3d^4 D_{5/2}^{\circ}$	981475	981130	...	...	1.182E-11	1.179E-11
28	97	$3s^2 S 3p^3 ({}^4S) {}^3S 3d^4 D_{7/2}^{\circ}$	982540	982195	...	...	1.266E-11	1.262E-11
28	98	$3s^2 S 3p^3 ({}^4S) {}^3S 3d^4 D_{1/2}^{\circ}$	983058	982713	...	...	1.192E-11	1.191E-11
28	99	$3s^2 S 3p^3 ({}^2D) {}^1D 3d^2 D_{3/2}^{\circ}$	987642	987297	...	...	1.377E-11	1.378E-11
28	100	$3s^2 S 3p^3 ({}^2D) {}^3D 3d^2 F_{5/2}^{\circ}$	993900	993555	...	...	1.454E-11	1.460E-11
28	101	$3s^2 S 3p^3 ({}^2P) {}^3P 3d^2 P_{1/2}^{\circ}$	995566	995221	...	...	1.712E-11	1.711E-11
28	102	$3s^2 S 3p^3 ({}^2D) {}^3D 3d^2 D_{5/2}^{\circ}$	997006	996661	...	...	1.423E-11	1.431E-11
28	103	$3s^2 S 3p^3 ({}^2D) {}^3D 3d^2 F_{7/2}^{\circ}$	1003694	1003349	...	...	1.234E-11	1.240E-11
28	104	$3s^2 S 3p^3 ({}^2P) {}^3P 3d^2 P_{3/2}^{\circ}$	1009094	1008749	...	...	2.539E-11	2.534E-11
28	105	$3s^2 3p^2 P 3d^2 ({}^3F) {}^4G_{5/2}^{\circ}$	1011058	1010713	...	...	2.889E-11	2.896E-11
28	106	$3s^2 3p^2 P 3d^2 ({}^3F) {}^4G_{7/2}^{\circ}$	1015318	1014973	...	...	3.205E-11	3.212E-11
28	107	$3s^2 S 3p^3 ({}^2P) {}^1P 3d^2 D_{3/2}^{\circ}$	1019286	1018941	...	...	1.369E-11	1.373E-11
28	108	$3s^2 3p^2 P 3d^2 ({}^3P) {}^2S_{1/2}^{\circ}$	1020981	1020636	...	...	1.087E-11	1.094E-11
28	109	$3s^2 3p^2 P 3d^2 ({}^3F) {}^4G_{9/2}^{\circ}$	1022136	1021791	...	...	4.219E-11	4.223E-11
28	110	$3s^2 S 3p^3 ({}^2P) {}^1P 3d^2 D_{5/2}^{\circ}$	1025176	1024831	...	...	1.392E-11	1.394E-11
28	111	$3s^2 3p^2 P 3d^2 ({}^1D) {}^2P_{3/2}^{\circ}$	1030497	1030152	...	...	8.268E-12	8.300E-12
28	112	$3s^2 S 3p^3 ({}^2P) {}^1P 3d^2 F_{5/2}^{\circ}$	1032640	1032295	...	...	1.346E-11	1.348E-11
28	113	$3s^2 3p^2 P 3d^2 ({}^3F) {}^4G_{11/2}^{\circ}$	1032931	1032586	...	...	4.393E-11	4.391E-11
28	114	$3s^2 S 3p^3 ({}^2P) {}^1P 3d^2 F_{7/2}^{\circ}$	1035028	1034683	...	...	1.367E-11	1.368E-11

Table 3 continued

Table 3 (continued)

Z	Key	Level	$E_{\text{CI1}}$	$E_{\text{CI2}}$	$E_{\text{NIST}}$	$E_{\text{MRMP}}$	$\tau_1$	$\tau_v$
28	115	$3s^2 3p^2 P 3d^2(^1D) 2P_{1/2}^{\circ}$	1045945	1045600	...	...	8.436E-12	8.474E-12
28	116	$3s^2 3p^2 P 3d^2(^3P) 4D_{1/2}^{\circ}$	1065442	1065097	...	...	1.624E-11	1.632E-11
28	117	$3s^2 3p^2 P 3d^2(^3P) 4D_{3/2}^{\circ}$	1067681	1067336	...	...	1.638E-11	1.646E-11
28	118	$3s^2 3p^2 P 3d^2(^3P) 4D_{5/2}^{\circ}$	1070506	1070161	...	...	1.480E-11	1.486E-11
28	119	$3s^2 3p^2 P 3d^2(^3P) 4D_{7/2}^{\circ}$	1078127	1077782	...	...	1.431E-11	1.437E-11
28	120	$3s^2 3p^2 P 3d^2(^1D) 2F_{5/2}^{\circ}$	1078328	1077983	...	...	1.350E-11	1.355E-11
28	121	$3s^2 S 3p^3(^2P) 1P 3d^2 2P_{3/2}^{\circ}$	1081784	1081439	...	...	8.623E-12	8.675E-12
28	122	$3s^2 3p^2 P 3d^2(^3F) 4F_{3/2}^{\circ}$	1082715	1082370	...	...	8.967E-12	9.004E-12
28	123	$3s^2 S 3p^3(^2P) 1P 3d^2 2P_{1/2}^{\circ}$	1084139	1083794	...	...	8.902E-12	8.957E-12
28	124	$3s^2 3p^2 P 3d^2(^3P) 4P_{1/2}^{\circ}$	1085769	1085424	...	...	1.328E-11	1.336E-11
28	125	$3s^2 3p^2 P 3d^2(^1G) 2H_{9/2}^{\circ}$	1085927	1085582	...	...	2.757E-11	2.771E-11
28	126	$3s^2 3p^2 P 3d^2(^3F) 4F_{5/2}^{\circ}$	1086265	1085920	...	...	9.209E-12	9.250E-12
28	127	$3s^2 3p^2 P 3d^2(^3P) 4P_{3/2}^{\circ}$	1091328	1090983	...	...	1.327E-11	1.334E-11
28	128	$3s^2 3p^2 P 3d^2(^3F) 4F_{7/2}^{\circ}$	1091356	1091011	...	...	9.827E-12	9.871E-12
28	129	$3s^2 3p^2 P 3d^2(^1D) 2F_{7/2}^{\circ}$	1092504	1092159	...	...	1.353E-11	1.358E-11
28	130	$3s^2 3p^2 P 3d^2(^3F) 4F_{9/2}^{\circ}$	1092913	1092568	...	...	9.813E-12	9.865E-12
28	131	$3s^2 3p^2 P 3d^2(^3F) 2D_{5/2}^{\circ}$	1097904	1097559	...	...	1.038E-11	1.041E-11
28	132	$3s^2 3p^2 P 3d^2(^1D) 2D_{3/2}^{\circ}$	1099783	1099438	...	...	1.097E-11	1.099E-11
28	133	$3s^2 3p^2 P 3d^2(^3P) 4P_{5/2}^{\circ}$	1102481	1102136	...	...	1.093E-11	1.098E-11
28	134	$3s^2 3p^2 P 3d^2(^1G) 2H_{11/2}^{\circ}$	1107847	1107502	...	...	3.245E-11	3.251E-11
28	135	$3s^2 3p^2 P 3d^2(^1G) 2G_{7/2}^{\circ}$	1111720	1111375	...	...	1.119E-11	1.122E-11
28	136	$3s^2 3p^2 P 3d^2(^1G) 2G_{9/2}^{\circ}$	1118792	1118447	...	...	1.164E-11	1.169E-11
28	137	$3s^2 S 3p^3(^4S) 3S 3d^2 D_{5/2}^{\circ}$	1126985	1126640	...	...	7.260E-12	7.307E-12
28	138	$3s^2 S 3p^3(^4S) 3S 3d^2 D_{3/2}^{\circ}$	1130286	1129941	...	...	6.400E-12	6.442E-12
28	139	$3s^2 3p^2 P 3d^2(^3F) 4D_{7/2}^{\circ}$	1133768	1133423	...	...	7.030E-12	7.069E-12
28	140	$3s^2 3p^2 P 3d^2(^3F) 4D_{5/2}^{\circ}$	1135396	1135051	...	...	7.001E-12	7.036E-12
28	141	$3s^2 3p^2 P 3d^2(^3F) 4D_{3/2}^{\circ}$	1137021	1136676	...	...	6.854E-12	6.884E-12
28	142	$3s^2 3p^2 P 3d^2(^3F) 4D_{1/2}^{\circ}$	1138048	1137703	...	...	6.687E-12	6.717E-12
28	143	$3s^2 S 3p^3(^2D) 1D 3d^2 S_{1/2}^{\circ}$	1139112	1138767	...	...	6.648E-12	6.680E-12

NOTE— Table 3 is published in its entirety in the machine-readable format. The values for  $Z = 28$  are shown here for guidance regarding its form and content.

**Table 4.** Comparison of excitation energies (in  $\text{cm}^{-1}$ ) for the lowest 41 levels Fe XII.  $E_{\text{CI2}}$  the present calculations where energies of excited states have been shifted by a constant  $ES$  given in Table 2 (see text for more details).  $E_{\text{NIST}}$  are the NIST energies.  $E_{\text{DM}}$  lists the observed energies recommended by [Del Zanna & Mason \(2005\)](#) (values in brackets indicate estimated energies), while  $E_{\text{CHI}}$  lists the observed energies as in the CHIANTI database version 8 ([Del Zanna et al. 2015](#); [Dere et al. 1997](#)). The superscript  $^{\circ}$  indicates energies that appear to be incorrect.  $\Delta E = E_{\text{CI2}} - E_{\text{CHI}}$ .

Key	Level	$E_{\text{CI2}}$	$E_{\text{NIST}}$	$E_{\text{DM}}$	$E_{\text{CHI}}$	$\Delta E$
1	$3s^2 3p^3(^4S) 4S_{3/2}^{\circ}$	0	0	0	0	0
2	$3s^2 3p^3(^2D) 2D_{3/2}^{\circ}$	41404	41566	41555	41555	-151
3	$3s^2 3p^3(^2D) 2D_{5/2}^{\circ}$	45952	46075	46088	46088	-136
4	$3s^2 3p^3(^2P) 2P_{1/2}^{\circ}$	74005	74372	74107	74107	-102
5	$3s^2 3p^3(^2P) 2P_{3/2}^{\circ}$	80395	80515	80515	80515	-120
6	$3s^2 S 3p^4(^3P) 4P_{5/2}$	274131	274373	274373	274373	-242
7	$3s^2 S 3p^4(^3P) 4P_{3/2}$	283759	284005	284005	284005	-246
8	$3s^2 S 3p^4(^3P) 4P_{1/2}$	288084	288307	288307	288307	-223

Table 4 continued



Table 4 (continued)

Key	Level	$E_{\text{CI2}}$	$E_{\text{NIST}}$	$E_{\text{DM}}$	$E_{\text{CHI}}$	$\Delta E$
9	$3s^2 S 3p^4(^1D) ^2D_{3/2}$	339737	340020	339725	339725	12
10	$3s^2 S 3p^4(^1D) ^2D_{5/2}$	341683	341703	341716	341716	-33
11	$3s^2 S 3p^4(^3P) ^2P_{3/2}$	389706	389706	389719	389719	-13
12	$3s^2 3p^2(^3P) ^3P 3d ^2P_{1/2}$	394345	394120	394360	394360	-15
13	$3s^2 S 3p^4(^1S) ^2S_{1/2}$	410447	...	410401	410401	46
14	$3s^2 3p^2(^3P) ^3P 3d ^4F_{3/2}$	426875	...	426920	427034	-159
15	$3s^2 3p^2(^3P) ^3P 3d ^4F_{5/2}$	430647	...	430758	430743	-96
16	$3s^2 3p^2(^3P) ^3P 3d ^4F_{7/2}$	436182	...	436088	436088	94
17	$3s^2 3p^2(^1D) ^1D 3d ^2F_{5/2}$	442756	...	(443318)	...	...
18	$3s^2 3p^2(^3P) ^3P 3d ^4F_{9/2}$	443013	...	443121	443121	-108
19	$3s^2 3p^2(^1D) ^1D 3d ^2F_{7/2}$	447045	...	447070	447070	-25
20	$3s^2 3p^2(^3P) ^3P 3d ^4D_{1/2}$	447334	...	(446977)	...	...
21	$3s^2 3p^2(^3P) ^3P 3d ^4D_{3/2}$	448390	...	(448071)	447076 <sup>o</sup>	1314
22	$3s^2 3p^2(^3P) ^3P 3d ^4D_{5/2}$	452671	...	451651 <sup>o</sup>	452755	-84
23	$3s^2 3p^2(^3P) ^3P 3d ^4D_{7/2}$	462024	...	461474	461474	550
24	$3s^2 3p^2(^1D) ^1D 3d ^2G_{7/2}$	494376	...	494518	494518	-142
25	$3s^2 3p^2(^1D) ^1D 3d ^2G_{9/2}$	497424	...	497256	497256	168
26	$3s^2 3p^2(^3P) ^3P 3d ^2P_{3/2}$	501838	501800	501800	501800	38
27	$3s^2 3p^2(^3P) ^3P 3d ^4P_{5/2}$	512390	512510	512508	512508	-118
28	$3s^2 S 3p^4(^3P) ^2P_{1/2}$	513907	513850	513850	513850	57
29	$3s^2 3p^2(^3P) ^3P 3d ^4P_{3/2}$	516670	516740	516772	516772	-102
30	$3s^2 3p^2(^3P) ^3P 3d ^4P_{1/2}$	519671	519770	519767	519767	-96
31	$3s^2 3p^2(^1S) ^1S 3d ^2D_{3/2}$	526350	526120	526127	526127	223
32	$3s^2 3p^2(^1S) ^1S 3d ^2D_{5/2}$	537118	538040 <sup>o</sup>	536939	536939	179
33	$3s^2 3p^2(^1D) ^1D 3d ^2D_{3/2}$	554046	554030	553906	553906	140
34	$3s^2 3p^2(^1D) ^1D 3d ^2D_{5/2}$	554811	554610	554632	554632	179
35	$3s^2 3p^2(^1D) ^1D 3d ^2P_{1/2}$	569932	568940 <sup>o</sup>	569794	569794	138
36	$3s^2 3p^2(^3P) ^3P 3d ^2F_{5/2}$	576944	576740	576733	576733	211
37	$3s^2 3p^2(^1D) ^1D 3d ^2P_{3/2}$	577823	577740	577680	577680	143
38	$3s^2 3p^2(^1D) ^1D 3d ^2S_{1/2}$	579827	579630	576153 <sup>o</sup>	576153 <sup>o</sup>	3674
39	$3s^2 3p^2(^3P) ^3P 3d ^2F_{7/2}$	581370	581180	581171	581171	199
40	$3s^2 3p^2(^3P) ^3P 3d ^2D_{5/2}$	604180	603930	603940	603940	240
41	$3s^2 3p^2(^3P) ^3P 3d ^2D_{3/2}$	605813	605480	605540	605540	273

**Table 5.** Transition wavelengths  $\lambda$  (in  $\text{\AA}$ ), transition rates  $A$  (in  $\text{s}^{-1}$ ), weighted oscillator strengths  $gf$  and line strengths  $S$  (in a.u.) between the lowest 143 states of Cr X, Mn XI, Fe XII, Co XIII, Ni XIV, Cu XV, Zn XVI. All transition data are in length form. Type is the type of the multipole, BF is the branching fraction from the upper level and  $dT$  is the relative difference of the transition rates in length and velocity form as given by Eq. (3). Only transitions with  $\text{BF} \geq 10^{-5}$  are presented.

$Z$	$i$	$j$	Type	$\lambda$	$A$	$gf$	$S$	BF	$dT$
24	1	2	M1	2.6802E+03	1.298E+01	5.591E-08	3.705E-02	9.984E-01	
24	1	2	E2	2.6802E+03	2.144E-02	9.238E-11	1.059E-02	1.650E-03	1.222E-03
24	1	3	M1	2.5205E+03	3.874E-01	2.214E-09	1.380E-03	6.900E-01	
24	1	3	E2	2.5205E+03	4.305E-02	2.460E-10	2.346E-02	7.667E-02	1.019E-03
24	2	3	M1	4.2302E+04	1.310E-01	2.109E-07	2.206E+00	2.333E-01	
24	1	4	M1	1.5579E+03	6.488E+01	4.722E-08	1.819E-02	6.999E-01	
24	1	4	E2	1.5579E+03	2.118E-02	1.541E-11	3.471E-04	2.285E-04	9.716E-04
24	2	4	M1	3.7203E+03	2.703E+01	1.122E-07	1.032E-01	2.915E-01	
24	2	4	E2	3.7203E+03	5.317E-01	2.206E-09	6.767E-01	5.735E-03	2.859E-02
24	3	4	E2	4.0791E+03	2.441E-01	1.218E-09	4.923E-01	2.633E-03	2.843E-02
24	1	5	M1	1.4835E+03	1.348E+02	1.779E-07	6.528E-02	6.003E-01	
24	2	5	M1	3.3227E+03	6.084E+01	4.028E-07	3.310E-01	2.709E-01	
24	2	5	E2	3.3227E+03	3.521E-01	2.331E-09	5.094E-01	1.568E-03	2.764E-02

Table 5 continued

Table 5 (continued)

$Z$	$i$	$j$	Type	$\lambda$	$A$	$gf$	$S$	BF	$dT$
24	3	5	M1	3.6060E+03	2.761E+01	2.153E-07	1.920E-01	1.229E-01	
24	3	5	E2	3.6060E+03	7.091E-01	5.529E-09	1.544E+00	3.157E-03	2.675E-02
24	4	5	M1	3.1091E+04	2.717E-01	1.575E-07	1.211E+00	1.210E-03	
24	1	6	E1	4.2735E+02	1.203E+09	1.976E-01	2.780E-01	9.879E-01	2.486E-02
24	2	6	E1	5.0841E+02	3.939E+06	9.158E-04	1.533E-03	3.235E-03	6.181E-02
24	3	6	E1	5.1460E+02	9.554E+06	2.276E-03	3.855E-03	7.848E-03	6.634E-02
24	5	6	E1	6.0026E+02	1.187E+06	3.847E-04	7.603E-04	9.751E-04	9.224E-02
24	1	7	E1	4.1650E+02	1.283E+09	1.334E-01	1.830E-01	9.950E-01	1.842E-02
24	2	7	E1	4.9314E+02	6.565E+05	9.574E-05	1.554E-04	5.092E-04	8.122E-02
24	3	7	E1	4.9895E+02	1.610E+06	2.403E-04	3.947E-04	1.249E-03	7.263E-02
24	4	7	E1	5.6849E+02	4.065E+04	7.878E-06	1.474E-05	3.153E-05	4.612E-02
24	5	7	E1	5.7908E+02	4.112E+06	8.270E-04	1.577E-03	3.190E-03	8.069E-02
24	1	8	E1	4.1144E+02	1.336E+09	6.782E-02	9.186E-02	9.956E-01	1.533E-02
24	2	8	E1	4.8606E+02	1.777E+06	1.259E-04	2.014E-04	1.324E-03	4.299E-02
24	4	8	E1	5.5910E+02	3.597E+06	3.371E-04	6.205E-04	2.680E-03	9.047E-02
24	5	8	E1	5.6934E+02	5.660E+05	5.501E-05	1.031E-04	4.217E-04	1.400E-01
24	1	9	E1	3.4487E+02	7.088E+05	5.055E-05	5.740E-05	2.656E-04	8.030E-03
24	2	9	E1	3.9580E+02	2.387E+09	2.243E-01	2.922E-01	8.944E-01	1.691E-02
24	3	9	E1	3.9954E+02	6.404E+07	6.131E-03	8.064E-03	2.399E-02	1.622E-03
24	4	9	E1	4.4292E+02	2.134E+08	2.511E-02	3.661E-02	7.995E-02	2.784E-02
24	5	9	E1	4.4932E+02	3.808E+06	4.610E-04	6.819E-04	1.427E-03	2.579E-02
24	1	10	E1	3.4371E+02	3.504E+06	3.723E-04	4.213E-04	1.413E-03	1.325E-03
24	2	10	E1	3.9428E+02	3.704E+07	5.179E-03	6.722E-03	1.494E-02	2.730E-02
24	3	10	E1	3.9799E+02	2.055E+09	2.928E-01	3.836E-01	8.289E-01	1.746E-02
24	5	10	E1	4.4736E+02	3.837E+08	6.908E-02	1.017E-01	1.548E-01	3.855E-02

NOTE— Table 5 is published in its entirety in the machine-readable format. Part of the values for  $Z = 24$  are shown here for guidance regarding its form and content.

**Table 6.** Transition wavelengths  $\lambda$  (in Å) and transition rates  $A$  (in  $\text{s}^{-1}$ ) for the brightest lines in Fe XII. Column 6 and 7 transition wavelengths and rates from this work, column 8 and 9 transition wavelengths and rates from [Del Zanna & Mason \(2005\)](#).  $\lambda_{CI}$  and  $A_{CI}$  are from this work,  $\lambda_{DZ}$  and  $A_{DZ}$  from [Del Zanna & Mason \(2005\)](#). Column 10 transition rates from NIST. This table is an adaptation of Table 3 from [Del Zanna & Mason \(2005\)](#).

$i$	$j$	lower level	upper level	Type	$\lambda_{CI}$	$A_{CI}$	$\lambda_{DZ}$	$A_{DZ}$	$A_{NIST}$
1	2	$3s^2 3p^3(4S) 4S_{3/2}^{\circ}$	$3s^2 3p^3(2D) 2D_{3/2}^{\circ}$	M1	2394.0	5.415E+01	2406.41 ± 0.06	5.6E+01	4.8E+01
1	3	$3s^2 3p^3(4S) 4S_{3/2}^{\circ}$	$3s^2 3p^3(2D) 2D_{5/2}^{\circ}$	M1	2158.9	2.071E+00	2169.76 ± 0.05	2.3E+00	1.7E+00
1	5	$3s^2 3p^3(4S) 4S_{3/2}^{\circ}$	$3s^2 3p^3(2P) 2P_{3/2}^{\circ}$	M1	1238.2	3.447E+02	1242.01 ± 0.01	3.5E+02	3.2E+02
1	4	$3s^2 3p^3(4S) 4S_{3/2}^{\circ}$	$3s^2 3p^3(2P) 2P_{1/2}^{\circ}$	M1	1344.6	1.888E+02	1349.40 ± 0.02	1.9E+02	1.8E+02
2	5	$3s^2 3p^3(2D) 2D_{3/2}^{\circ}$	$3s^2 3p^3(2P) 2P_{3/2}^{\circ}$	M1	2564.7	1.978E+02	2566.77 ± 0.13	2.0E+02	2.0E+02
3	5	$3s^2 3p^3(2D) 2D_{5/2}^{\circ}$	$3s^2 3p^3(2P) 2P_{3/2}^{\circ}$	M1	2903.4	7.923E+01	2904.70 ± 0.17	8.2E+01	...
2	4	$3s^2 3p^3(2D) 2D_{3/2}^{\circ}$	$3s^2 3p^3(2P) 2P_{1/2}^{\circ}$	M1	3067.3	7.005E+01	3072.06 ± 0.19	7.2E+01	...
18	25	$3s^2 3p^2(3P) 3P 3d^4 F_{9/2}$	$3s^2 3p^2(1D) 1D 3d^2 G_{9/2}$	M1	1837.8	1.176E+02	1847.23 ± 11.19	1.2E+02	...
16	18	$3s^2 3p^2(3P) 3P 3d^4 F_{7/2}$	$3s^2 3p^2(3P) 3P 3d^4 F_{9/2}$	M1	14639	8.077E+00	14218.68 ± 258.05	1.2E+01	...
6	18	$3s^2 S 3p^4(3P) 4P_{5/2}$	$3s^2 3p^2(3P) 3P 3d^4 F_{9/2}$	E2	592.13	5.606E+01	592.600 ± 0.123	6.2E+01	...
1	6	$3s^2 3p^3(4S) 4S_{3/2}^{\circ}$	$3s^2 S 3p^4(3P) 4P_{5/2}$	E1	364.30	1.597E+09	364.467 ± 0.007	1.7E+09	1.6E+09
1	7	$3s^2 3p^3(4S) 4S_{3/2}^{\circ}$	$3s^2 S 3p^4(3P) 4P_{3/2}$	E1	351.96	1.752E+09	352.106 ± 0.006	1.8E+09	1.7E+09
1	8	$3s^2 3p^3(4S) 4S_{3/2}^{\circ}$	$3s^2 S 3p^4(3P) 4P_{1/2}$	E1	346.68	1.851E+09	346.852 ± 0.006	1.9E+09	1.8E+09
3	11	$3s^2 3p^3(2D) 2D_{5/2}^{\circ}$	$3s^2 S 3p^4(3P) 2P_{3/2}$	E1	290.91	7.556E+09	291.010 ± 0.018	7.8E+09	...
3	10	$3s^2 3p^3(2D) 2D_{5/2}^{\circ}$	$3s^2 S 3p^4(1D) 2D_{5/2}$	E1	338.15	2.746E+09	338.263 ± 0.013	2.9E+09	2.9E+09
2	9	$3s^2 3p^3(2D) 2D_{3/2}^{\circ}$	$3s^2 S 3p^4(1D) 2D_{3/2}$	E1	335.20	3.342E+09	335.380 ± 0.035	3.5E+09	3.5E+09
2	12	$3s^2 3p^3(2D) 2D_{3/2}^{\circ}$	$3s^2 3p^2(3P) 3P 3d^2 P_{1/2}$	E1	283.33	7.176E+09	283.443 ± 0.017	7.4E+09	...
5	13	$3s^2 3p^3(2P) 2P_{3/2}^{\circ}$	$3s^2 S 3p^4(1S) 2S_{1/2}$	E1	302.98	7.136E+09	303.135 ± 0.019	7.5E+09	...
1	27	$3s^2 3p^3(4S) 4S_{3/2}^{\circ}$	$3s^2 3p^2(3P) 3P 3d^4 P_{5/2}$	E1	195.02	8.264E+10	195.119 ± 0.002	8.5E+10	8.6E+10
1	29	$3s^2 3p^3(4S) 4S_{3/2}^{\circ}$	$3s^2 3p^2(3P) 3P 3d^4 P_{3/2}$	E1	193.41	8.448E+10	193.509 ± 0.002	8.7E+10	9.1E+10
1	30	$3s^2 3p^3(4S) 4S_{3/2}^{\circ}$	$3s^2 3p^2(3P) 3P 3d^4 P_{1/2}$	E1	192.29	8.297E+10	192.394 ± 0.002	8.7E+10	9.0E+10

Table 6 continued

Table 6 (continued)

$i$	$j$	lower level	upper level	Type	$\lambda_{CI}$	$A_{CI}$	$\lambda_{DZ}$	$A_{DZ}$	$A_{NIST}$
3	39	$3s^2 3p^3(^2D) 2D_{5/2}^{\circ}$	$3s^2 3p^2(^3P) 3P 3d^2 F_{7/2}$	E1	186.77	1.040E+11	$186.887 \pm 0.007$	1.1E+11	1.0E+11
3	32	$3s^2 3p^3(^2D) 2D_{5/2}^{\circ}$	$3s^2 3p^2(^1S) 1S 3d^2 D_{5/2}$	E1	203.60	2.876E+10	$203.728 \pm 0.005$	2.9E+10	...
3	16	$3s^2 3p^3(^2D) 2D_{5/2}^{\circ}$	$3s^2 3p^2(^3P) 3P 3d^4 F_{7/2}$	E1	256.26	2.676E+07	$256.410 \pm 0.066$	2.4E+07	...
3	19	$3s^2 3p^3(^2D) 2D_{5/2}^{\circ}$	$3s^2 3p^2(^1D) 1D 3d^2 F_{7/2}$	E1	249.32	3.262E+07	$249.388 \pm 0.032$	3.1E+07	...
3	34	$3s^2 3p^3(^2D) 2D_{5/2}^{\circ}$	$3s^2 3p^2(^1D) 1D 3d^2 D_{5/2}$	E1	196.52	3.951E+10	$196.640 \pm 0.002$	4.1E+10	4.9E+10
1	22	$3s^2 3p^3(^4S) 4S_{3/2}^{\circ}$	$3s^2 3p^2(^3P) 3P 3d^4 D_{5/2}$	E1	220.73	3.661E+08	$221.410 \pm 0.049$	3.1E+08	...
3	23	$3s^2 3p^3(^2D) 2D_{5/2}^{\circ}$	$3s^2 3p^2(^3P) 3P 3d^4 D_{7/2}$	E1	240.34	4.996E+05	$240.740 \pm 0.059$	1.8E+05	...
3	26	$3s^2 3p^3(^2D) 2D_{5/2}^{\circ}$	$3s^2 3p^2(^3P) 3P 3d^2 P_{3/2}$	E1	219.35	4.344E+10	$219.437 \pm 0.015$	4.5E+10	...
3	27	$3s^2 3p^3(^2D) 2D_{5/2}^{\circ}$	$3s^2 3p^2(^3P) 3P 3d^4 P_{5/2}$	E1	214.39	1.345E+09	$214.399 \pm 0.003$	1.4E+09	1.1E+09
2	30	$3s^2 3p^3(^2D) 2D_{3/2}^{\circ}$	$3s^2 3p^2(^3P) 3P 3d^4 P_{1/2}$	E1	209.09	4.908E+09	$209.113 \pm 0.003$	4.2E+09	1.8E+09
1	17	$3s^2 3p^3(^4S) 4S_{3/2}^{\circ}$	$3s^2 3p^2(^1D) 1D 3d^2 F_{5/2}$	E1	225.67	9.734E+07	$225.572 \pm 0.254$	1.1E+08	...
2	14	$3s^2 3p^3(^2D) 2D_{3/2}^{\circ}$	$3s^2 3p^2(^3P) 3P 3d^4 F_{3/2}$	E1	259.42	1.612E+08	$259.495 \pm 0.068$	1.7E+08	...
2	31	$3s^2 3p^3(^2D) 2D_{3/2}^{\circ}$	$3s^2 3p^2(^1S) 1S 3d^2 D_{3/2}$	E1	206.21	7.723E+09	$206.368 \pm 0.005$	8.2E+09	...
2	36	$3s^2 3p^3(^2D) 2D_{3/2}^{\circ}$	$3s^2 3p^2(^3P) 3P 3d^2 F_{5/2}$	E1	186.73	9.696E+10	$186.854 \pm 0.004$	9.9E+10	...
5	40	$3s^2 3p^3(^2P) 2P_{3/2}^{\circ}$	$3s^2 3p^2(^3P) 3P 3d^2 D_{5/2}$	E1	190.92	8.909E+10	$191.049 \pm 0.008$	9.0E+10	...
2	33	$3s^2 3p^3(^2D) 2D_{3/2}^{\circ}$	$3s^2 3p^2(^1D) 1D 3d^2 D_{3/2}$	E1	195.07	5.634E+10	$195.179 \pm 0.002$	5.7E+10	6.1E+10
3	24	$3s^2 3p^3(^2D) 2D_{5/2}^{\circ}$	$3s^2 3p^2(^1D) 1D 3d^2 G_{7/2}$	E1	223.00	2.714E+08	$223.000 \pm 0.100$	2.5E+08	...
5	37	$3s^2 3p^3(^2P) 2P_{3/2}^{\circ}$	$3s^2 3p^2(^1D) 1D 3d^2 P_{3/2}$	E1	201.03	5.043E+10	$201.140 \pm 0.008$	5.1E+10	5.1E+10
2	34	$3s^2 3p^3(^2D) 2D_{3/2}^{\circ}$	$3s^2 3p^2(^1D) 1D 3d^2 D_{5/2}$	E1	194.78	2.582E+09	$194.903 \pm 0.002$	2.2E+09	1.7E+09
3	33	$3s^2 3p^3(^2D) 2D_{5/2}^{\circ}$	$3s^2 3p^2(^1D) 1D 3d^2 D_{3/2}$	E1	196.81	9.331E+09	$196.921 \pm 0.002$	9.7E+09	1.1E+09
4	37	$3s^2 3p^3(^2P) 2P_{1/2}^{\circ}$	$3s^2 3p^2(^1D) 1D 3d^2 P_{3/2}$	E1	198.48	1.759E+10	$198.581 \pm 0.008$	1.9E+10	1.6E+10
4	33	$3s^2 3p^3(^2P) 2P_{1/2}^{\circ}$	$3s^2 3p^2(^1D) 1D 3d^2 D_{3/2}$	E1	208.32	5.697E+09	$208.421 \pm 0.003$	6.2E+09	6.7E+09
6	84	$3s^2 S 3p^4(^3P) 4P_{5/2}$	$3s^2 S 3p^3(^2P) 3P 3d^4 D_{7/2}^{\circ}$	E1	186.73	6.985E+10	$191.007 \pm 0.184$	6.8E+10	...

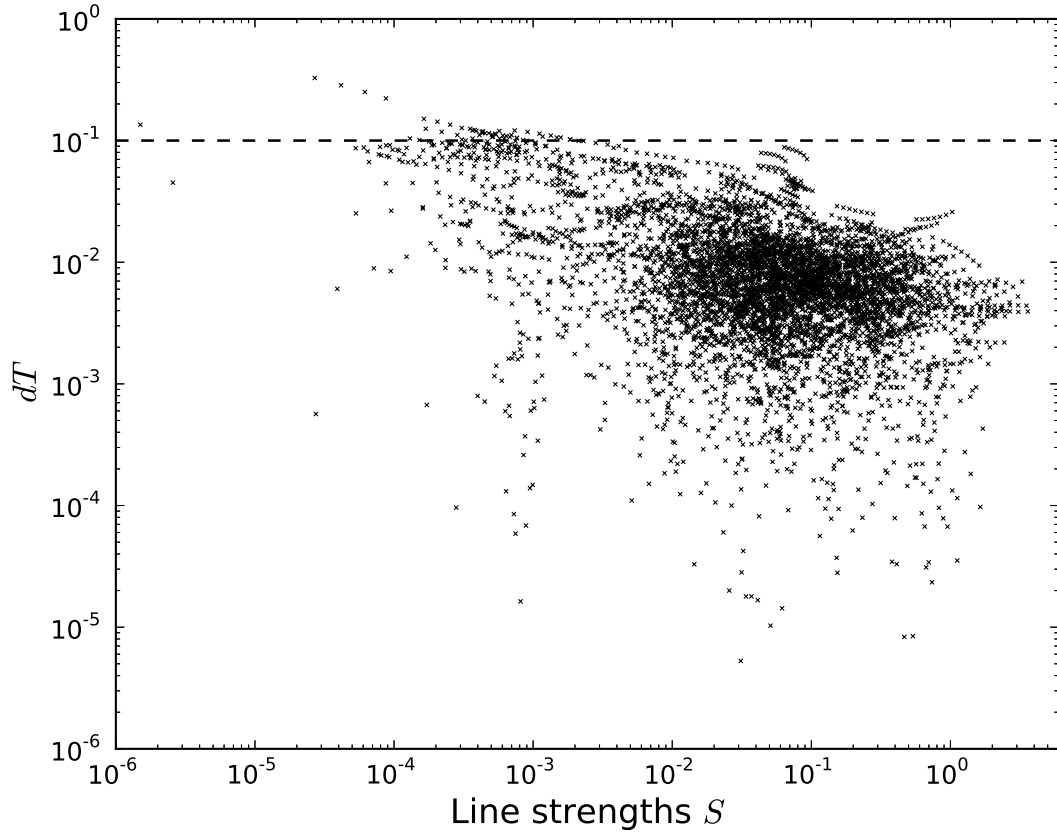


**Figure 1.** Scatter plot of  $dT$ , the relative difference between the transition rates in length and velocity form, versus the line strength  $S$  for transitions in Fe XII with branching fractions  $\text{BF} > 1\%$ .  $dT$  is well below 5% for the majority of the stronger transitions.